A MASS SPECTROMETRIC STUDY OF SOME TRIFLUOROPHOSPHINE-SUBSTITUTED TRANSITION METAL CARBONYLS

by

MARIA ANN KRASSOI

B. S., Notre Dame College, 1965

A MASTER'S THESIS

submitted in partial fulfillment of the

requirements for the degree

MASTER OF SCIENCE

Department of Chemistry

KANSAS STATE UNIVERSITY
Manhattan, Kansas

1968

Approved by:

Major Professor

TABLE OF CONTENTS

		Page
LIST OF FIGURES		iii
LIST OF TABLES		iv
I.	INTRODUCTION	1
	A. Statement of Problem	1
	B. Previous Studies	2
II.	EXPERIMENTAL	6
	A. Instrumentation	6
	B. Data Reduction	8
	C. Materials	10
III.	ENERGETIC DATA AND METASTABLE TRANSITIONS	12
	A. Appearance Potentials	12
	B. Metastables	14
IV.	TRIFLUOROPHOSPHINE COMPLEXES OF TRANSITION METALS	20
	A. Trifluorophosphine-Substituted Carbonyls of Molybdenum	20
	1. Mass Spectra	20
	2. Clastograms	26
	3. Energetic Studies	32
	B. Tetrakis(trifluorophosphine)nickel(0)	38
	1. Mass Spectra	38
	2. Clastograms	41
	3. Energetic Studies	45
	C. Tetrakis(trifluorophosphine)cobalt(I)hydride	48
	1. Mass Spectra	48
	2. Clastograms	48
	3. Energetic Studies	51
V.	SUMMARY	54
VI.	ACKNOWLEDGMENTS	56
VII.	LITERATURE CITED	57

Page

APPENDICES 61

A. Tabulation of Data for Metastable Transition Calculations Using the Bendix Time-of-Flight Mass Spectrometer. 62

B. Heat of Formation (in kcal/mole) for the Molecules, Atoms, Ions and Radicals used in the Thermochemical Calculations. . 67

C. Tabulation of Heats of Formation (in kcal/mole) of Ionic Species Studied. 68

ABSTRACT

LIST OF FIGURES

		Page
Figure 1.	Metastable Transitions in Tetrakis(trifluorophosphine)-nickel(0).	18
Figure 2.	Clastogram for Hexakis- and Carbonylpentakis-(trifluorophosphine)molybdenum(0)	28
Figure 3.	Clastogram for cis-Tetracarbonylbis(trifluorophosphine)-molybdenum(0).	29
Figure 4.	Clastogram for trans-Tetracarbonylbis(trifluoro-phosphine)molybdenum(0).	30
Figure 5.	Clastogram for Pentacarbonyl(trifluorophosphine)-molybdenum(0).	31
Figure 6.	Clastogram for Tetrakis(trifluorophosphine)nickel(0) . . .	42
Figure 7.	Clastogram for the Less Abundant Ions of Tetrakis-(trifluorophosphine)nickel(0).	44
Figure 8.	Clastogram for Tetrakis(trifluorophosphine)cobalt(I)-hydride	50

LIST OF TABLES

		Page
Table 1.	Names and Formulas of Compounds Investigated	3
Table 2.	Metastable Transitions in Tetrakis(trifluorophosphine)nickel(0)	19
Table 3.	Relative Abundances of the Principal Ions from Hexakis- and Carbonylpentakis(trifluorophosphine)-molybdenum(0)	21
Table 4.	Relative Abundances of the Principal Ions from Pentacarbonyl(trifluorophosphine)molybdenum(0)	22
Table 5.	Relative Abundances of the Principal Ions from cis- and trans-Tetracarbonylbis(trifluorophosphine)-molybdenum(0)	23
Table 6.	Relative Abundances of the Doubly-Charged Ions from trans-Tetracarbonylbis(trifluorophosphine)-molybdenum(0)	24
Table 7.	Appearance Potentials and Heats of Formation of the Principal Positive Ions of Pentacarbonyl(trifluorophosphine)molybdenum(0)	35
Table 8.	Appearance Potentials and Heats of Formation of the Principal Positive Ions of cis-Tetracarbonylbis-(trifluorophosphine)molybdenum(0)	36
Table 9.	Appearance Potentials and Heats of Formation of the Principal Positive Ions of trans-Tetracarbonylbis-(trifluorophosphine)molybdenum(0)	37
Table 10.	Relative Abundances of the Principal Ions from Tetrakis(trifluorophosphine)nickel(0)	39
Table 11.	Appearance Potentials and Heats of Formation of the Principal Positive Ions of Tetrakis(trifluorophosphine)-nickel(0)	47
Table 12.	Relative Abundances of the Principal Ions from Tetrakis(trifluorophosphine)cobalt(I)hydride.	49

Page

Table 13. Appearance Potentials and Heats of Formation of the Principal Positive Ions of Tetrakis(trifluorophosphine)cobalt(I)hydride 52

Table 14. $410^+ \rightarrow 332^+ + 88$ Metastable Transition in Tetrakis(trifluorophosphine)nickel(0). 63

Table 15. $332^+ \rightarrow 234^+ + 88$ Metastable Transition in Tetrakis(trifluorophosphine)nickel(0). 64

Table 16. $234^+ \rightarrow 146^+ + 88$ Metastable Transition in Tetrakis(trifluorophosphine)nickel(0). 65

Table 17. $391^+ + 410 \rightarrow 410^+ + 391^+$ Charge Exchange in Tetrakis(trifluorophosphine)nickel(0). 66

I. INTRODUCTION

The behavior of organometallic compounds under electron impact, particularly those of the metal carbonyls and organosubstituted metal carbonyls, has been investigated (5,15,40,57,58,59,60,61,62,64). These studies provide a source of thermochemical information for ions, radicals and molecules, as well as give information as to the structure and bond character of these organometallics. While there have been a few mass spectrometric investigations on mixed-ligand compounds, no systematic studies as yet have been made on compounds in which some or all of the organic ligands have been replaced by inorganic groups. For this reason, studies have been initiated on various trifluorophosphine-substituted transition metal carbonyls.

A. Statement of Problem

Since PF_3 and CO are rather different molecules, but yet bond to transition metals in similar fashion, it was of interest to examine the behavior of compounds containing these ligands under electron impact using mass spectrometry. The questions to be considered are the following: (i) In the ionization of these molecules, is it possible to determine whether the electron removed was originally associated with the ligand or with the metal? (ii) Does dissociative ionization occur in a stepwise fashion or competitively? (iii) Which bond ruptures first in these molecules? (iv) Is there ligand dissociation, i.e., P-F

and C-O bond rupture, prior to detachment of the ligand from the central metal atom? If there is, how extensive is this process? (v) How do the fragmentation patterns of cis and trans isomers compare? (vi) On mass spectrometric evidence alone, can any prediction be made as to the thermal stability of the cis and trans isomers? (vii) How do the relative abundances of the ions compare in the mass spectrum obtained on the Bendix 12-100 time-of-flight and the Hitachi RMU-6E double-focusing mass spectrometers? (viii) Is there any evidence of production of multiply-charged ions from these compounds?, and (ix) Can any prediction be made as to the bonding tendencies of PF_3 and CO groups to the transition metals from these results?

In order to answer the preceding questions, mass spectrometric data has been determined for a series of trifluorophosphine metal carbonyls; these are listed in Table 1.

B. Previous Studies

The mass spectra, ionization and appearance potentials, clastograms and heats of formation of several transition metal carbonyls and some substituted metal carbonyls have been studied in detail (5,15,40,56,57). More recently, attention has been focused on the mixed-ligand compounds in which an organic group has been replaced by an inorganic ligand. Examples of this group of organometallics which have been studied by mass spectrometry include the carbonyl hydrides, nitrosyls, halides and thiols.

Rhomberg and Owen (42) reported that the mass spectrum of the product of the reaction of $Cr(CO)_6$ and alcoholic potassium hydroxide

Table 1. Names and Formulas of Compounds Investigated

Name	Formula
Hexakis(trifluorophosphine)molybdenum(0)	$Mo(PF_3)_6$
Carbonylpentakis(trifluorophosphine)-molybdenum(0)	$MoCO(PF_3)_5$
cis- and trans-Tetracarbonylbis-(trifluorophosphine)molybdenum(0)	$Mo(CO)_4(PF_3)_2$
Pentacarbonyl(trifluorophosphine)-molybdenum(0)	$Mo(CO)_5PF_3$
Tetrakis(trifluorophosphine)nickel(0)	$Ni(PF_3)_4$
Tetrakis(trifluorophosphine)cobalt(I)hydride	$HCo(PF_3)_4$

was consistent with $H_2Cr(CO)_4$. In characterizing $H_nRu_4(CO)_{12}$ from their preparations, Jamienson, Kingston and Wilkinson (21) found the highest m/q to be 754, which corresponded to $H_2Ru_4(CO)_{12}^+$. The presence of four ruthenium atoms in the molecule was further indicated by the Ru_4^+ ion. No definite implications as to the structure could be made on mass spectral evidence alone; however, these authors suggest the possible bonding of the hydrogen atoms to the faces of a ruthenium tetrahedron having terminal CO groups.

Edgell and Risen (13) observed a doublet of peaks separated by 28 atomic mass units in the mass spectrum of $HMn(CO)_5$. These peaks correspond to metal carbonyl and metal carbonyl hydride ions. Due to an intense MnH^+ peak, direct metal-hydrogen bonding was suggested; this was confirmed by infrared studies (13). A direct relationship between the intensities of singly- and doubly-charged ions was also noted, similar to the findings of Winters and Kiser (63). It was suggested by Edgell and Risen (13) that a competitive loss of CO groups and H atoms occurs, but Johnson, et al. (22) cite no evidence for this in their investigations of several carbonyl hydrides. In cyclopentadienyl molybdenum dicarbonyl nitrosyl, it was found (62) that the CO groups are removed in preference to the NO and C_5H_5 groups and that the ionization potential is intermediate between the ionization potentials of molybdenum, nitric oxide and the cyclopentadienyl radical. From the mass spectra of halogen- and thiol-bridged nitrosyl complexes of iron and cobalt, Johnson, et al. (23) established a dimeric structure in the gas phase and noted the stability of the metal-sulfur ring structure.

The principal loss of CO groups and halogen atoms has been noted by Edgar, et al. (12) in the mass spectra of monomeric metal carbonyl halides.

The halogen-bridged dimers of manganese, rhenium and rhodium and the related thiol-bridged compounds of iron, rhenium and manganese were observed to lose carbonyl groups preferentially with the preservation of the M_2X_2 or M_2S_2 nucleus. Evidence for tetrameric compounds was also found (12).

Studies on substituted phosphine carbonyls and phosphine- and sulfur-bridged binuclear carbonyls have concentrated mostly on mass spectra and metastables. Lewis, et al. (34) noted the expected, successive elimination of CO groups in $(C_6H_5)_3PMo(CO)_5$ and $(C_6H_5)_3PW(CO)_5$. More recently the reaction products between tetraphenylcyclotetraphosphine and transition metals (1) and some tris(dimethylamino)phosphine metal carbonyls (26) have also been studied by mass spectrometry.

The behavior of tetrakis(trifluorophosphine)nickel(0) under electron impact has been studied (30) and found to be similar to that of $Ni(CO)_4$ (58). The absence of doubly-charged ions in the $Ni(PF_3)_4$ mass spectrum suggests that the bonding in $Ni(PF_3)_4$ is different to some extent from the bonding in the carbonyl analogue.

II. EXPERIMENTAL

The instruments employed in this study were a Bendix model 12-100 linear time-of-flight mass spectrometer and a Hitachi model RMU-6E double-focusing high resolution mass spectrometer. The theory and instrumental modifications of time-of-flight mass spectrometers have been reported previously (4,18,24,36,37,53,54,65) as well as the details of the particular instrument used in this study (9,10,17,19,20,46,49,52,56). Since no major modifications have been done on the former instrument, only the basic principles of operation will be discussed. Due to its limited use, only the instrumental setup of the Hitachi RMU-6E double-focusing mass spectrometer will be given.

A. Instrumentation

In the ion source of the Bendix time-of-flight mass spectrometer, the gaseous sample is ionized by bombardment with electrons which are generated by heating a 5 mil tungsten filament with approximately 3.5 amperes of current. This ionizing beam of electrons is collimated both mechanically and magnetically and is pulsed by applying a positive potential to a slit located between the filament and the ionization region. The variation of potential between this slit and the d.c. filament determines the energy of the electrons. This energy is displayed on a Hewlett-Packard 3440A (8) digital voltmeter. By the application of a constant positive potential to a trapping anode, the electrons are drawn through the ionization region. The average electron current at this anode was measured to be approximately 0.13 microamperes.

The master pulse, operated at 10 kilohertz produces 10,000 mass spectra per second. The ions formed in the ionization chamber are drawn out by a potential of -270 v at 90° to the electron beam and then further accelerated through a potential drop of -2800 volts. After this, the ions enter a field-free drift tube with a flight path of approximately one meter. Since all the ions are given the same momentum, their velocities will vary as the square root of their mass-to-charge ratios (thus the heavier ions will arrive later at the detector than the lighter ions). Assuming that all the ions leave the source at approximately the same time, ions of the same m/q will bunch together and be separated from those of different m/q ratios. As each group of ions arrives at the detector, secondary electrons are released and multiplied in mutually perpendicular magnetic and electric fields of the Wiley magnetic electron multiplier (54). The resulting electrons are then brought to the oscilloscope anode and the signal amplified and displayed on a Hewlett-Packard model 175A oscilloscope. The mass spectrum is traced on heat sensitive "Permapaper" by a Sanborn model 152 dual-channel recording system.

The resolution, by the $2.08\Gamma_{\frac{1}{2}}$ definition (27) was approximately 130. Although no resolution of the transition metal isotopes in the metal-trifluorophosphine carbonyl ions of mass greater than 200 was obtained, there was no difficulty in identifying the ions since they were separated at least by 19 atomic mass units, i.e., at least by a fluorine atom.

Liquid, as well as solid samples were vaporized in an 8-cm. long glass tube which was attached to a Kovar seal. The metal end of the seal was connected to a Hoke Model 2PY280 stainless steel needle valve to control the sample flow. Apiezon "N" grease was used on all joints. No external heating was necessary, since all the samples had sufficient vapor pressures

at room temperature. Operating pressures were about 2-5 x 10^{-6} torr and were maintained by a mechanical forepump and a mercury diffusion pump with liquid nitrogen trap and baffles.

No appreciable thermal decomposition was noted during these studies, although the source and detector required periodic cleaning due to metal deposits. This was accomplished by immersing the source and detector components in 12% HF solution in a Sonblaster ultrasonic cleaner (47). Periodic replacement of the tungsten filament was also necessary; however, results were reproducible with the different filaments.

The Hitachi RMU-6E double-focusing mass spectrometer consists of a Nier-type ion source, an electrostatic sector with a 45° deflection angle and a radius of curvature of 250 mm, followed by a magnetic sector with a deflection angle of 90° and a 200 mm radius of curvature and an electron multiplier detector with a gain of 10^4-10^6. The magnetic field is variable manually or automatically between 400 and 7500 gauss. The accelerating voltages employed were either 3600 or 1800 volts, depending on the mass range of interest, (300 or 600 amu, respectively), and its resolution is better than 10,000 based on the $2.08\Gamma_{\frac{1}{2}}$ definition (27).

B. Data Reduction

The mass spectra reported here were taken at electron energies of 70 ev. In calculating the relative abundances of the ions, the most intense metal-containing peak is referred to as the "base peak" and is assigned the relative abundance of 100%. The abundances of all other peaks are calculated in reference to this base peak. Due to the limited resolution of the time-of-flight instrument, only the most abundant isotope of each metal was utilized in the relative abundance calculations (after its separation from overlapping peaks).

Ionization and appearance potentials were acquired by the energy compensation method (29) which involves the centering of one "gate" of the electron multiplier on the ions studied and the other on a calibrant ion, mercury (IP = 10.43 ev), used in these studies. The ion currents then were recorded on separate channels of the dual-channel recorder at 50 ev. The sensitivity was then increased 100-fold and the electron energy decreased until the ion current intensity read the same for each ion as previously at 50 ev. The difference in voltages is the difference in the appearance potentials of the two ions. In the case of compounds with several isotopes, the gate was centered on the most abundant isotope.

Clastograms were obtained by scanning the entire mass spectrum at 70 ev, then decreasing the electron energy by 10,5,2,1, and finally 0.5 ev increments and recording the mass spectrum at each energy. At low energies smaller increments are taken since the decrease of the ion current is very rapid. The clastogram itself is the plot of the fractional abundance of an ion as the function of electron energy (27).

Three general types of fragmentation curves are notable in most clastogram plots. The parent-molecule ion, or one behaving as one, starts out with a fractional abundance of nearly unity at low electron energies, decreases rapidly and finally levels off above about 50 ev. A second curve is the type that reaches a maximum usually between 15 and 30 ev, then decreases and levels off. This type of behavior is indicative of a consecutive decomposition process (31), where the ion originates from some other species, then decomposes into simpler ions. Finally, there are curves which simply "grown in", i.e., their fractional abundance

increases continuously with electron energy. These curves usually represent terminal processes where further fragmentation does not occur. These curves are represented in the clastograms of trans-$Mo(CO)_4(PF_3)_2$ (see Figure 4, for example).

C. Materials

The metal trifluorophosphines utilized in this study were kindly furnished by Dr. R. J. Clark of Florida State University. Each of the samples was introduced into the mass spectrometer without further purification since no evidence of appreciable amounts of impurities were noted in the time-of-flight mass spectrum. Small traces of tungsten-containing species were found in the high resolution mass spectrum of cis- and trans-tetracarbonylbis(trifluorophosphine)molybdenum(0) and pentacarbonyl(trifluorophosphine)molybdenum(0).

Tetrakis(trifluorophosphine)nickel(0), $Ni(PF_3)_4$, was prepared approximately as described earlier (6). About 2 g. of $Ni(CO)_4$ was vacuum distilled into a 150 ml stainless steel pressure vessel along with a quantity of purified (7) PF_3 adequate to yield a pressure of 300 p.s.i. at room temperature. The vessel was heated to 125-150° for 12 hours, then cooled to -195° and the CO that was formed was removed by vacuum. This was continued through about four cycles until the amount of CO formed in the successive steps was approaching the point of diminishing return.

The product was a mixture of about 80% $Ni(PF_3)_4$ and 20% $NiCO(PF_3)_3$ and no more than a trace of any of the other trifluorophosphine nickel carbonyl species. The tetraphosphine was isolated by preparative scale

gas-liquid chromatography using an Autoprep A-700 gas chromatograph. A 7.5 m x ¼ in. column of 40% DC-702 silicone oil on Kromat FB was used with helium as the carrier at a flow of about 60 cc per minute. Temperatures of 25-40° were satisfactory using injections of about 30 µl. The product, which was trapped at -78°, was dried by vacuum distillation through a bed of 4A molecular sieves. The product was chromatographically pure when tested by glpc on an analytical scale and was found by low voltage mass spectrometry to contain no discernible impurities.

III. ENERGETIC DATA AND METASTABLE TRANSITIONS

As stated previously, electron impact studies provide a basis for thermochemical calculations and for the determination of fragmentation processes for gaseous ions and molecules. Metastable transitions also provide information about fragmentation processes. These are briefly discussed in the following paragraphs.

A. Appearance Potentials

Mass spectrometric energetics deal with the determination of ionization and appearance potentials. The appearance potential is the energy required to form a fragment ion and its accompanying neutral products in their ground states. A special case of the appearance potential is the ionization potential, in which process an electron is ejected from the highest occupied molecular orbital, without further fragmentation of the molecular ion.

Ionization effected by electron impact is a vertical process as required by the Franck-Condon principle (14) and therefore the resulting ion may or may not be in its ground state as is the case in spectroscopic methods. As a result, ionization potentials measured by mass spectrometry may be higher than those found spectroscopically (28).

The appearance potential is the measure of the heat of reaction for a process such as shown in Equation 1,

$$XY + e \rightarrow X^+ + Y + 2e \qquad (1)$$

and may be expressed as

$$A(X^+) = \Delta H_f(X^+) + \Delta H_f(Y) - \Delta H_f(XY) + E(X^+) + E(Y) - E(XY) + KE(X^+) + KE(Y) - KE(XY) \qquad (2)$$

where: $A(X^+)$ is the minimum energy required to form X^+

ΔH_f is the heat of formation of the gaseous species enclosed in parentheses,

E is the excess internal energy and

KE is the kinetic energy of the fragment ion and neutral species.

The internal energy and kinetic energy of the molecule, at the temperature of operation of the TOF mass spectrometer ($\sim$40°C) is negligible to other energies involved, so Equation 2 may be simplified to

$$A(H^+) = \Delta H_f(X^+) + \Delta H_f(Y) - \Delta H_f(XY) + E(X^+) + E(Y) + KE(X^+) + KE(Y). \quad (3)$$

Further, assuming that the ion and the neutral fragments are formed in their ground states with no excess kinetic energy, Equation 3 may be rewritten as

$$A(X^+) = \Delta H_f(X^+) + \Delta H_f(Y) - \Delta H_f(XY). \quad (4)$$

The approximations made above are necessary, since time-of-flight mass spectrometry does not normally provide for the measurement of these energies. Previous studies (14) have validated the above approximations in many cases.

The heats of formation of the various gaseous ions may now be calculated from the heat of formation of the molecule and neutral fragments, and the appearance potential of the ion.

The final value of the appearance potential is usually arrived at by the averaging of the values from the Warren (51), linear extrapolation (48), semi-log (35) and the energy compensation (29) methods. Since instrumental difficulties in this work prevented the acquisition of "long form" appearance potentials which are to be employed in the Warren, linear extrapolation and semi-log calculations, only the energy compensation method (29) results are reported and used in this investigation.

B. Metastables

Metastable studies are invaluable in the assignment of decomposition processess. Since the conventional time-of-flight mass spectrometer is not equipped to give such information, certain modifications were made (11) to enable the detection of metastable transitions. The following derivation by Prof. R. W. Kiser gives a semi-quantitative method for the identification of the mass of the daughter ions resulting from such a transition.

If an ion of mass m_o and charge q is accelerated from zero velocity through a potential drop of V_a to a velocity of v_o, its kinetic energy will be

$$KE_1 = m_o v_o^2/2 = qV_a \tag{5}$$

Its velocity in a field-free region is

$$v_o = (2qV_a/m_o)^{\frac{1}{2}} \tag{6}$$

If at some point in the flight the mother ion decomposes to form a daughter ion of mass m and charge q, and a neutral fragment of mass $(m_o - m)$, the velocity of both remains v_o, so that both will arrive at the detector at the same time as any undecomposed ion with a mass-to-charge ratio of m_o/q. Therefore, metastables with half-lives on the order of 10^{-5} to 10^{-7} seconds will not be observed. If, however, a retarding field is imposed upon all ions after leaving the field-free region, but prior to reaching the detector, the daughter ion may be separated from the mother ion on the basis of their kinetic energy differences.

Prior to retardation, the kinetic energy of the daughter ion is

$$KE_2 = mv_o^2/2 = (m/m_o)qV_a \tag{7}$$

which becomes

$$KE = KE_2 - qV_r \tag{8}$$

after the application of a retarding field of V_r. This may also be expressed as

$$KE = KE_2 - q(V_a - V_s) \tag{9}$$

where V_s is the potential on the stack of the multiplier. From the kinetic energy expression

$$KE = mv^2/2 = (m/m_o)qV_a - qV_a + qV_s \tag{10}$$

or

$$KE = mv^2/2 = (m - m_o)qV_a/m_o + qV_s \tag{11}$$

the velocity may be calculated to be

$$v = [2qV_s/m - 2(\Delta m)qV_a/m_o m]^{\frac{1}{2}} \tag{12}$$

where $\Delta m = (m_o - m)$ is the mass of the neutral fragment.

The flight time of the ions of mass m_o and m in the field free field before retardation is $t_2 = d_2/v_o$, while after retardation in a field of length d_4, it is

$$t_4 = d_4 [2qV_s/m - 2(\Delta m)qV_a/m_o m]^{-\frac{1}{2}} \tag{13}$$

and therefore

$$t_4^{-2} = [2qV_s - 2(\Delta m)qV_a/m_o]/d_4^2 m \tag{14}$$

or

$$1/t_4^2 = 2qV_s/d_4^2 m = 2(\Delta m)qV_a/d_4^2 m_o m. \tag{15}$$

In the above equation d_4 and V_a are constants, and m_o, m, Δm and q are constants in a given metastable transition. Therefore, Equation 15 may be simplified to

$$1/t_4^2 = kV_s - K \tag{16}$$

where

$$k = 2q/d_4^2 m \tag{17}$$

and

$$K = 2(\Delta m)qV_a/d_4^2 m_o m = k(\Delta m)V_a/m_o. \quad (18)$$

Consequently, a plot of $1/t_4^2$ versus V_s should give a straight line of slope = k and intercept = -K.

In order to determine the mass of the daughter ion resulting from a metastable transition, Equation 17 may be used, but first a specific value of t_4 must be found.

The flight time of ions not subjected to retardation is

$$t = d(m/2qV)^{\frac{1}{2}}. \quad (19)$$

The difference in the flight times of two ions of mass m_1 and m_2 having the same charge q is

$$t = (t_2 - t_1) = [d/(2qV)^{\frac{1}{2}}][m_2^{\frac{1}{2}} - m_1^{\frac{1}{2}}] \quad (20)$$

In this study, d = 100 cm, q = 4.803×10^{-10} esu, V = 3000 volts and m_1 and m_2 are in atomic mass units. Therefore,

$$t = 1.315(m_2^{\frac{1}{2}} - m_1^{\frac{1}{2}}) \text{ microseconds.} \quad (21)$$

By the selection of two ions, the difference in the flight times and distances on the chart paper can be determined, which gives a distance-time calibration of $(\Delta t/\Delta l)$.

From the distance shifts on the chart paper, the retardation of any daughter ion may be determined as the function of V_s. Any additional time spent in the d_4 retardation region is denoted by t_s and when this is added to $t_4°$, the normal flight time of the mother ion of the metastable transition, t_4 is obtained:

$$t_4 = t_4° + t_s \quad (22)$$

t_4 may be calculated from Equation 19 by replacing m with m_o.

Having arrived at the necessary parameters, the plot of $1/t_4^2$ versus V_s should yield a straight line of slope k and intercept K. When $1/t_4^2 = 0$, let $V_s = V_s^o$ and Equation 16 gives $K = kV_s^o$ or

$$V_s^o = K/k. \tag{23}$$

From Equation 18,

$$K/k = (m_o - m)V_a/m_o \tag{24}$$

which becomes

$$(m_o - m)/m_o = V_s^o/V_a = (1 - m/m_o) \tag{25}$$

when V_s^o is substituted for K/k. Now solving for the mass of the daughter ion, one obtains

$$m = m_o(V_a - V_s^o)/V_a \tag{26}$$

The four metastable transitions observed in $Ni(PF_3)_4$ are shown in Figure 1. The masses of the daughter ions were determined both from the slope and the intercept by a least square treatment, the details of which are shown in Appendix A. The results are summarized in Table 2. The unique transition $391^+ \rightarrow 410^+$ will be explained in detail in section IV. B. 3.

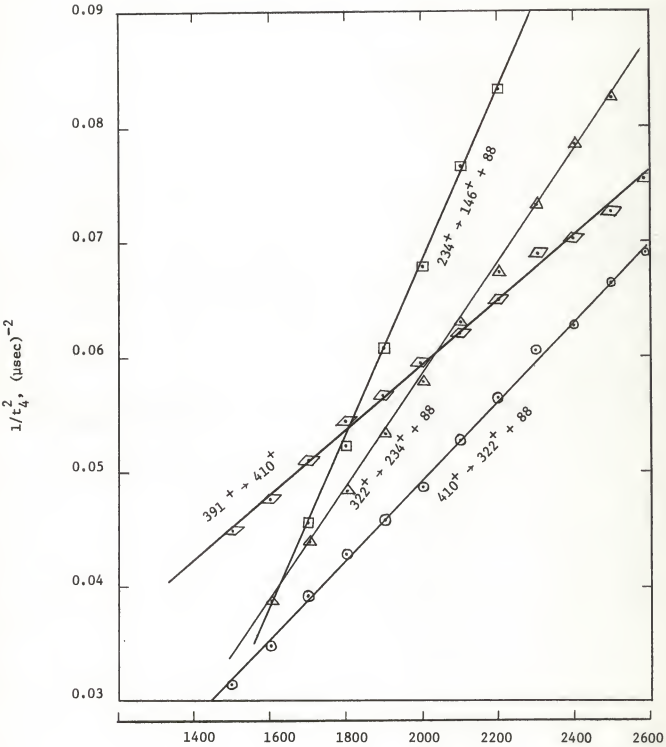

Figure 1. Metastable Transitions in Tetrakis(trifluorophosphine)-nickel(0).

Table 2. Metastable Transitions in Tetrakis(trifluorophosphine)-nickel(0).

Mother Ion (amu)	Daughter Ion (amu)			
	from slope	from intercept	average	assignment
410	337.8	332	335	322
322	237.8	235.4	236	234
234	150.9	147.2	149	146
391	414	405.5	410	410

IV. TRIFLUOROPHOSPHINE COMPLEXES OF TRANSITION METALS

The experimental data obtained on a mixture of hexakis- and carbonylpentakis-(trifluorophosphine)molybdenum(0), cis- and trans-tetracarbonylbis(trifluorophosphine)molybdenum(0), pentacarbonyl-(trifluorophosphine)molybdenum(0), tetrakis(trifluorophosphine)-nickel(0), and tetrakis(trifluorophosphine)cobalt(I)hydride, is presented in this section. The positive ion mass spectra, clastograms and appearance potentials for the major metal-containing species are discussed and their heats of formation calculated. Where possible, comparison is made of the behavior of the unsubstituted and the trifluorophosphine-substituted transition metal carbonyls.

A. Trifluorophosphine-Substituted Carbonyls of Molybdenum

1. Mass Spectra

The high resolution and time-of-flight monoisotopic mass spectra of the trifluorophosphine-substituted molybdenum carbonyl compounds are listed in Tables 3-6. The relative abundances of the time-of-flight mass spectra were based on the most abundant metal isotope, since resolution was not sufficient to enable the identification of the less abundant isotopes; complete analyses were made of the data obtained from the high resolution instrument. Overlapping peaks in the high resolution mass spectra were separated either by solving simultaneous equations or determinants, depending on the number of species contributing to the peak(s).

Table 3. Monoisotopic Relative Abundances of the Principal Ions from Hexakis- and Carbonylpentakis-(trifluorophosphine)molybdenum(0).

Ion	70 ev Relative Abundance	
	Time-of-flight	RMU-6E
Mo^+	100.0	99.4
$MoCO^+$	4.8	8.6
$MoCOPF_3^+$	3.8	14.4
$MoCO(PF_3)_2^+$	2.7	6.5
$MoCO(PF_3)_3^+$	0.9	6.8
$MoCO(PF_3)_4^+$	0.4	2.7
$MoCO(PF_3)_5^+$	1.9	4.7
$MoPF_3^+$	83.8	100.0
$Mo(PF_3)_2^+$	24.6	30.0
$Mo(PF_3)_3^+$	12.3	21.0
$Mo(PF_3)_4^+$	3.9	9.0
$Mo(PF_3)_5^+$	0.8	3.9
$Mo(PF_3)_6^+$	7.1	8.0
$MoPF_2^+$	16.1	30.6
$MoPF_3PF_2^+$	4.2	12.5
$Mo(PF_3)_2PF_2^+$	4.9	13.1
$Mo(PF_3)_3PF_2^+$	2.8	9.3
$Mo(PF_3)_4PF_2^+$	3.7	10.9
$Mo(PF_3)_5PF_2^+$	2.5	1.1
$MoPF^+$	6.6	17.5
MoP^+	?	11.3
MoF^+	36.1	62.0
MoF_2^+	4.1	14.3

Table 4. Monoisotopic Relative Abundances of the Principal Ions from Pentacarbonyl(trifluorophosphine)-molybdenum(0).

Ion	70 ev Relative Abundance	
	Time-of-flight	RMU-6E
Mo^+	100.0	87.0
$MoCO^+$	80.7	84.9
$Mo(CO)_2^+$	57.4	92.3
$Mo(CO)_3^+$	59.4	100.0
$Mo(CO)_4^+$	17.6	22.6
$Mo(CO)_5^+$	13.3	9.4
$MoPF_3^+$	9.0	11.3
$MoCOPF^+$	13.5	14.3
$Mo(CO)_3PF_3^+$	12.5	26.6
$Mo(CO)_2PF_3^+$	5.5	10.5
$Mo(CO)_3PF_3^+$	2.1	6.1
$Mo(CO)_5PF_3^+$	23.7	83.1
MoC^+	22.8	18.1
MoF^+	12.4	12.7
$MoPF_2^+$	?	3.1
$MoCOPF_2^+$	?	3.2
$Mo(CO)_2PF_2^+$	?	3.2
$Mo(CO)_3PF_2^+$	?	4.9
$Mo(CO)_4PF_2^+$	3.7	10.1
$Mo(CO)_5PF_2^+$	?	4.5
Mo^{++}	?	0.9
$MoCO^{++}$	5.7	3.9
$Mo(CO)_2^{++}$	3.7	2.9
$Mo(CO)_3^{++}$	?	1.9
$Mo(CO)_4^{++}$	?	0.6

Table 5. Monoisotopic Relative Abundances of the Principal Ions from cis- and trans-Tetracarbonylbis(trifluorophosphine)molybdenum(0).

	70 ev Relative Abundance			
	cis-		trans-	
Ion	TOF*	RMU-6E	TOF	RMU-6E
Mo^+	100.0	100.0	100.0	100.0
$MoCO^+$	60.2	50.3	68.3	55.2
$Mo(CO)_2^+$	31.9	31.1	48.0	33.7
$Mo(CO)_3^+$	22.7	14.2	25.3	21.3
$Mo(CO)_4^+$	5.3	1.1	9.7	3.9
$MoPF_3^+$	10.8	20.9	22.2	15.8
$MoCOPF_3^+$	7.9	13.8	15.7	10.1
$Mo(CO)_2PF_3^+$	12.4	12.7	28.8	11.4
$Mo(CO)_3PF_3^+$	6.8	0.4	12.2	3.0
$Mo(CO)_4PF_3^+$	1.5	0.6	3.6	0.8
MoC^+	15.7	27.6	21.5	19.3
MoF^+	17.2	32.2	27.3	27.8
MoF_2^+	3.9	6.6	5.4	6.4
$MoPF_2^+$	3.9	5.5	7.3	5.3
$MoCOPF_2^+$	2.4	4.2	4.8	2.1
$Mo(CO)_2PF_2^+$	1.8	2.9	4.6	2.1
$Mo(CO)_3PF_2^{2+}$	1.4	1.8	3.6	1.5
$Mo(CO)_4PF_2^{2+}$	0.8	?	7.0	1.4
$Mo(PF_3)_2^+$	?	?	5.3	0.8
$MoCO(PF_3)_2^+$	?	0.9	2.2	3.1
$Mo(CO)_2(PF_3)_2^+$	0.7	2.1	2.8	0.9
$Mo(CO)_3(PF_3)_2^{2+}$	?	0.3	1.8	0.3
$Mo(CO)_4(PF_3)_2^{2+}$	8.1	1.2	21.3	1.7

* Time-of-flight

Table 6. Monoisotopic Relative Abundances of the Doubly-Charged Ions from trans-Tetracarbonylbis-(trifluorophosphine)molybdenum(0).

	70 ev Relative Abundance	
Ion	Time-of-Flight	RMU-6E
Mo^{++}	2.1	0.6
$MoCO^{++}$	?	1.9
$Mo(CO)_2^{++}$	4.5	1.4
$Mo(CO)_3^{++}$	1.5	0.8
$MoPF_3^{++}$	?	0.2
$Mo(PF_3)_2^{++}$ or $MoCPF_3^{++}$	?	0.4

No previous mass spectrometric studies have been done on these compounds, although the cracking patterns and energetics of the analogous molybdenum hexacarbonyl have been examined (59).

As in $Mo(CO)_6$ (59), the most abundant positive ions fragmented from all the molybdenum compounds are the metal and the monocarbonyl metal ions. In general, the trifluorophosphine-containing species are lower in abundance than the carbonyl fragments, indicating a preferential removal of the PF_3 molecule. No pronounced differences exist between the time-of-flight and the high resolution mass spectra, although the abundance of the parent-molecule ions of cis- and trans-$Mo(CO)_4(PF_3)_2$ is about the same in the Hitachi and are in a one-to-three ratio in the time-of-flight mass spectra. The TOF result is not surprising if attributed to the inherent stability of trans structures in general. Comparison of the relative abundances of $Mo(CO)_5PF_3$ and cis- and trans-$Mo(CO)_4(PF_3)_2$ seems to indicate a decrease in abundance of the parent-molecule ion as a function of the degree of PF_3 substitution. This observation supports the previous proposition of preferential removal of the PF_3 ligand.

The existence of MoC^+, $MoPF_2^+$ and ions of the type $Mo(CO)_x(PF_3)_yPF_2^+$, where x = 0, 1, . . . , 4 and y = 0 or 1, indicates that ligand degradation does occur to some extent prior to detachment from the central metal. Judging from the relative abundances of these ions, the extent of this process is considerably less than the straight-forward M-PF_3 bond dissociation.

The parent and some of the fragment ions can also lose fluorophosphine fragments such as PF and PF_2, resulting in the formation of rearrangement ions containing Mo-F bonds. For example, loss of PF and

PF_2 from $MoPF_3^+$ results in MoF_2^+ (6.4% of the base peak) and MoF^+ (27.8% of the base peak) in trans-$Mo(CO)_4(PF_3)_2$.

A few doubly-charged ions also appear in significant quantities in the mass spectra of $Mo(CO)_5PF_3$ and trans-$Mo(CO)_4(PF_3)_2$, but not in the penta-hexa mixture or in the cis-$Mo(CO)_4(PF_2)_3$. These ions are extremely abundant compared to the usually encountered relative abundance of approximately 0.01 to 0.1% of the base peak (3,13,14) for most organic and some inorganic compounds. In his carbonyl studies, Winters (56) noted the unusually high abundance of the doubly-charged ions.

Of the five ions possessing two positive charges found in $Mo(CO)_5PF_3$, only two, $MoCO^{++}$ and $Mo(CO)_2^{++}$, are intense enough to be detectable on the time-of-flight mass spectrometer. In trans-$Mo(CO)_4(PF_3)_2$, two of the six doubly-charged ions had PF_3 present as a substituent, while PF_3 was absent in all the doubly-charged ions of $Mo(CO)_5PF_3$. One would expect to observe these same ions in the cis isomer, perhaps in lower abundance, but none was found. As in the case of the singly-charged ions, the relative abundances of the doubly-charged ions seem to decrease with increased PF_3 substitution.

2. Clastograms

The variation of fractional abundance as the function of electron energy, in graphical representation, is a clastogram (27). When the logarithm of the fractional abundance is plotted as a function of electron energy, the resulting curves are called clastologs, which are preferable for the presentation of data when the fractional abundance of an ion is extremely small.

Clastograms for the molybdenum compounds studied are shown in Figures 2-5. The compounds are arranged as they were previously in the mass spectra, and for clarity, the clastograms of cis- and trans-$Mo(CO)_4(PF_3)_2$ are divided into two parts, those in which PF_3 groups are present and those in which only CO groups appear. Such fragmentation curves give an indication of how a given ion may further dissociate to form a new ion and a neutral fragment. As noted before, three types of curves predominate in most clastograms (25); (i) curves which start out at a fractional abundance of almost unity and decrease rapidly as a function of electron energy, leveling off as the energy is further increased; (ii) curves which rise rapidly at low electron energies, reach a maximum usually between 15 and 30 electron volts, and then decrease slowly to a constant value with further increase in electron energy; and (iii) curves which gradually increase to a constant value.

Curves of type (i) are usually the parent-molecule ion. The fractional abundance of the various fragment ions may vary according to either curves (ii) or (iii). Primary processes, such as those in which a fragment ion may be formed directly from the parent-molecule ion at low appearance potentials, give rise to curves of type (ii); ions produced by more complex processes such as a fragment ion in turn decomposing to yield other fragments of lower m/q, or those that arise in a high energy process from the parent-molecule ion, exhibit curves of type (iii).

The types of curves described above have been observed in several organic and inorganic compounds (19,20,49,56). As in the unsubstituted transition metal carbonyls (56), curves of type (ii) display the same behavior; they "grow-in" and "peak" in order of their appearance potentials. The "peaking" tendency is indicative of a consecutive uni-

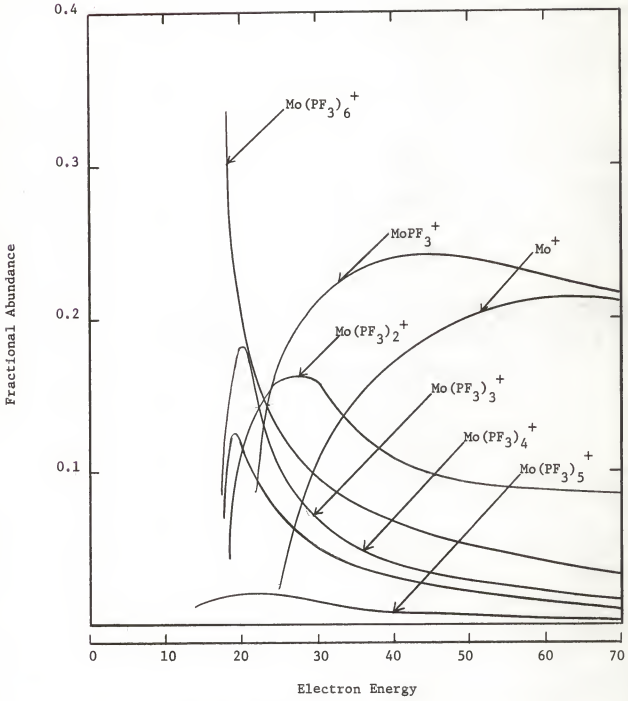

Figure 2. Clastogram of Hexakis- and Carbonylpentakis(trifluorophosphine)molybdenum(0).

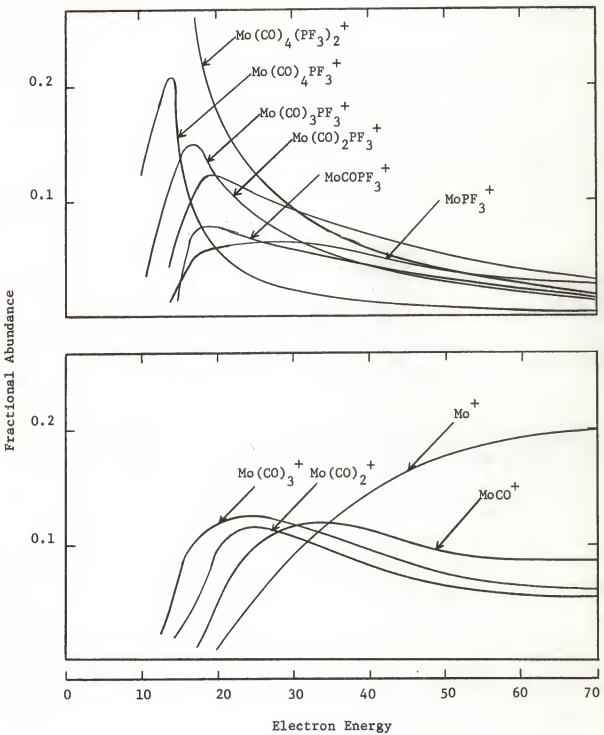

Figure 3. Clastogram of cis-Tetracarbonylbis(trifluorophosphine)-molybdenum(0).

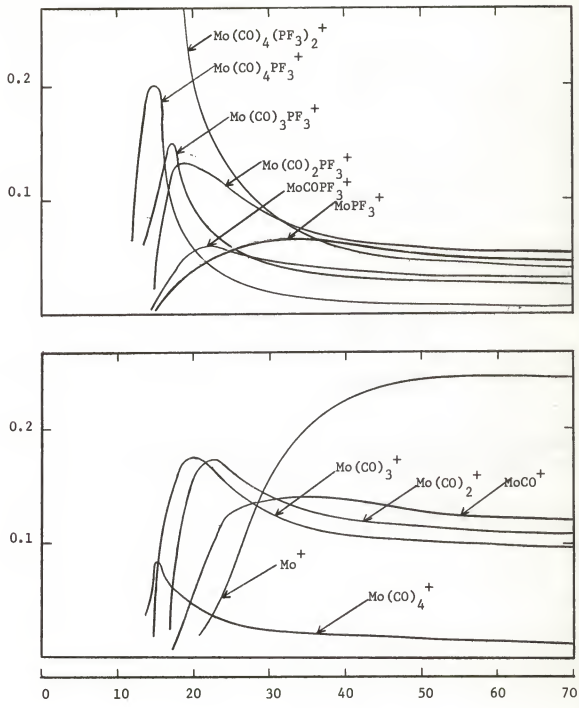

Figure 4. Clastogram of trans-Tetracarbonylbis(trifluorophosphine)-molybdenum(0).

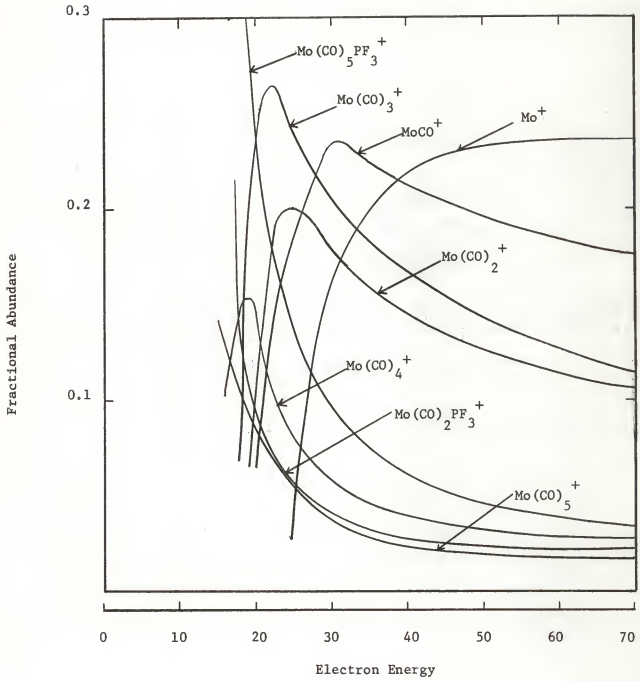

Figure 5. Clastogram of Pentacarbonyl(trifluorophosphine)-molybdenum(0).

molecular reaction, e.g.,

$$Mo(PF_3)_6^+ \rightarrow Mo(PF_3)_5^+ \rightarrow Mo(PF_3)_4^+ \rightarrow Mo(PF_3)_3^+ \rightarrow Mo(PF_3)_2^+ \rightarrow MoPF_3^+ \rightarrow Mo^+$$

Additionally, the clastograms of the cis- and trans-$Mo(CO)_4(PF_3)_2$ show that a PF_3 group is removed first, followed by the consecutive fragmentation of the carbonyl groups and finally by the removal of the second trifluorophosphine ligand. Examining these curves further, one notices that the maxima of the PF_3-containing species are much sharper than those for the carbonyls. This would indicate that the fractional abundance of the PF_3-containing fragments varies more rapidly with changes in energy than ions of the type $M(CO)_n^+$.

3. Energetic Studies

The minimum energy required for the formation of the major metal-containing ions in the mass spectra of the trifluorophosphine-substituted molybdenum carbonyls is summarized in Tables 7-9. The ions are listed according to decreasing m/q, followed by their appearance potentials, the probable processess by which they form and the calculated heats of formation. The heats of formation for the gaseous positive ions were calculated using the thermochemical data for the gaseous molecules, radicals and ions tabulated in Appendix B, and the mass spectrometrically determined appearance potentials.

The ionization potentials of cis- and trans-tetracarbonylbis-(trifluorophosphine)molybdenum(0) are 8.9 $\pm$ 0.2 ev and 8.8 $\pm$ 0.2 ev, respectively. These values are new, as well as the value of 8.8 $\pm$ 0.2 ev for the ionization potential of $Mo(CO)_5PF_3$. The low intensity of the

parent-molecule ion of $Mo(PF_3)_6$ prevented the determination of its ionization potential, but it is expected to be close to the above-mentioned values. According to these results, there is no significant difference between the ionization potentials of the cis and trans isomers, nor between the mono- and di-PF_3-substituted molybdenum carbonyls.

Since the above discussed ionization potentials are only slightly higher than the ionization potential of the metal atom (38), and considerably lower than the ionization potentials of the ligands (10,27), the electron withdrawn upon ionization may be considered to have been localized on the metal atom, rather than on the carbonyl or trifluorophosphine groups. From the low ionization potentials of the carbonyls, Winters (56) and Foffani, et al. (15) likewise argued that the electron withdrawn during ionization comes from the metal atom.

Energetic studies further indicate that the various $M(CO)_x(PF_3)_y^+$ ions fragmented from the PF_3-substituted carbonyls are formed by successive removal of neutral CO and PF_3 groups as shown below:

$$M(CO)_x(PF_3)_y + e \rightarrow M(CO)_{x-m}(PF_3)_{y-n}^+ + mCO + nPF_3 + 2e \qquad (28)$$

The low abundance of ions of the type $M(CO)_x(PF_3)_2^+$ and the greater abundance of $M(CO)_xPF_3^+$ ions suggests that the first PF_3 is removed in preference to all other ligands, while the second one is more difficult to detach than the carbonyl groups.

The heats of formation of the different ionic species from the various molybdenum compounds were calculated from the heat of formation of the parent molecule and neutral fragments. Since the heats of formation of the parent molecules were not available from the literature,

they were calculated from the heats of formation of the carbonyl fragments from molybdenum hexacarbonyl (56).

The appearance potential of an ion is equal to or greater than the heat of reaction by which it is formed. Assuming that $Mo(CO)_2^+$ forms from cis-$Mo(CO)_4(PF_3)_2$ by the following process,

$$Mo(CO)_4(PF_3)_2 + e \rightarrow Mo(CO)_2^+ + 2CO + 2PF_3 + 2e \quad (29)$$

its heat of reaction is

$$\Delta H_{rxn} = \Delta H_f Mo(CO)_2^+ + 2\Delta H_f(CO) + 2\Delta H_f(PF_3) - \Delta H_f(PM). \quad (30)$$

Further assuming that the heat of formation of $Mo(CO)_2^+$ involves the same, if any, excess energy in formation from cis-$Mo(CO)_4(PF_3)_2$ and $Mo(CO)_6$, and taking -26.4 and -219.6 kcal/mole for the heats of formation of CO and PF_3 respectively, the heat of formation of the parent molecule is calculated to be -595 kcal/mole. This method was used also in the estimation of the heats of formation for each of the other molybdenum compounds. Substitution of these heats of formation for the parent molecules and neutral ligands in Equation 4 yielded the thermochemical values listed in Tables 7-9, and in Appendix C.

No previous mass spectrometric or thermochemical information was available on hexakis- and carbonylpentakis-(trifluorophosphine)molybdenum-(0), the heats of formation of the parent molecules were calculated by assuming that every PF_3 substituted for a CO stabilizes the molecule by approximately 193 kcal/mole, i.e., the difference between the heats of formation of PF_3 and CO. A value of -400 kcal/mole was obtained for the heat of formation of $Mo(CO)_5PF_3$ by the above described method. If the

Table 7. Appearance Potentials and Heats of Formation of the Principal Positive Ions of Pentacarbonyl-(trifluorophosphine)molybdenum(0).

Ion	Appearance Potential (ev)	Probable Process	ΔH_f(ion) (kcal/mole)
$Mo(CO)_5PF_3^+$	8.8 ± 0.2	$Mo(CO)_5PF_3 \rightarrow Mo(CO)_5PF_3^+$	-197
$Mo(CO)_5^+$	11.3 ± 0.2	$\rightarrow Mo(CO)_5^+ + PF_3$	80
$Mo(CO)_4^+$	11.7 ± 0.2	$\rightarrow Mo(CO)_4^+ + CO + PF_3$	116
$Mo(CO)_3^+$	13.5 ± 0.2	$\rightarrow Mo(CO)_3^+ + 2CO + PF_3$	184
$Mo(CO)_2^+$	14.9 ± 0.2	$\rightarrow Mo(CO)_2^+ + 3CO + PF_3$	242
$MoCO^+$	16.7 ± 0.2	$\rightarrow MoCO^+ + 4CO + PF_3$	313
Mo^+	18.5 ± 0.3	$\rightarrow Mo^+ + 5CO + PF_3$	385

Table 8. Appearance Potentials and Heats of Formation of the Principal Positive Ions of cis-Tetracarbonylbis-(trifluorophosphine)molybdenum(0).

Ion	Appearance Potential (ev)	Probable Process	ΔH_f^+(ion) (kcal/mole)
$Mo(CO)_4(PF_3)_2^+$	8.9 ± 0.2	$Mo(CO)_4(PF_3)_2 \rightarrow Mo(CO)_4(PF_3)_2^+$	-390
$Mo(CO)_3PF_3^+$	12.0 ± 0.2	$\rightarrow Mo(CO)_3PF_3^+ + CO + PF_3$	- 72
$Mo(CO)_2PF_3^+$	13.5 ± 0.2	$\rightarrow Mo(CO)_2PF_3^+ + 2CO + PF_3$	- 11
$Mo(CO)_3^+$	13.8 ± 0.3	$\rightarrow Mo(CO)_3^+ + CO + 2PF_3$	189
$Mo(CO)_2^+$	15.2 ± 0.2	$\rightarrow Mo(CO)_2^+ + 2CO + 2PF_3$	248
$MoCO^+$	16.8 ± 0.4	$\rightarrow MoCO^+ + 3CO + 2PF_3$	311
Mo^+	18.5 ± 0.8	$\rightarrow Mo^+ 4CO + 2PF_3$	376

Table 9. Appearance Potentials and Heats of Formation of the Principal Positive Ions of trans-Tetracarbonylbis-(trifluorophosphine)molybdenum(0).

Ion	Appearance Potential (ev)	Probable Process	ΔH_f^+(ion) (kcal/mole)
$Mo(CO)_4(PF_3)_2^+$	8.8 ± 0.2	$Mo(CO)_4(PF_3)_2 \rightarrow Mo(CO)_4(PF_3)_2^+$	-392
$Mo(CO)_3PF_3^+$	12.1 ± 0.2	$\rightarrow Mo(CO)_3PF_3^+ + CO + PF_3$	- 70
$Mo(CO)_2PF_3^+$	13.8 ± 0.2	$\rightarrow Mo(CO)_2PF_3^+ + 2CO + PF_3$	- 5
$Mo(CO)_4^+$	12.3 ± 0.2	$\rightarrow Mo(CO)_4^+ + 2PF_3$	128
$Mo(CO)_3^+$	13.8 ± 0.2	$\rightarrow Mo(CO)_3^+ + CO + 2PF_3$	189
$Mo(CO)_2^+$	14.9 ± 0.2	$\rightarrow Mo(CO)_2^+ + 2CO + 2PF_3$	241
$MoCO^+$	16.8 ± 0.4	$\rightarrow MoCO^+ + 3CO + 2PF_3$	311
Mo^+	18.0 ± 0.6	$\rightarrow Mo^+ + 4CO + 2PF_3$	365

carbonyls are replaced by trifluorophosphine groups in succession, and if each PF_3 stabilizes the molecule by 193 kcal/mole, the heats of formation of $MoCO(PF_3)_5$ and $Mo(PF_3)_6$ are given by Equations 31 and 32

$$\Delta H_f[MoCO(PF_3)_5] = \Delta H_f[Mo(CO)_5PF_3] + 4[\Delta H_f(PF_3) - \Delta H_f(CO)] \quad (31)$$

$$H_f[Mo(PF_3)_6] = \Delta H_f[Mo(CO)_5PF_3] + 5[\Delta H_f(PF_3) - \Delta H_f(CO)] \quad (32)$$

and were estimated to be -1175 and -1365 kcal/mole, respectively.

The appearance potentials determined for the molybdenum metal ions yield heats of formation which are considerably greater than the presently accepted value of 327 kcal/mole (43). The difference between the experimentally determined heats of formation and the literature value is too great to be attributable to kinetic energies. This excess energy has been explained (56) to be the result of the formation of the metal ions in excited states which depend on the electronic configuration originally present in the molecule. If appropriate corrections are made for this excess energy, the resulting heats of formation are within approximately 20 kcal/mole of the presently accepted values (43).

Due to the very low vapor pressures, no appearance potentials were obtained or heats of formation calculated for the doubly-charged species.

B. Tetrakis(trifluorophosphine)nickel(0)

1. Mass Spectra

Only the time-of-flight 70 ev mass spectrum (monoisotopic) has been determined for this compound and it is given in Table 10. In the relative abundance calculations, only the nickel-58 isotope was used since resolution was not sufficient to permit the identification of all the

Table 10. Monoisotopic Relative Abundances of the Principal Ions from Tetrakis(trifluorophosphine)nickel(0).

Ion	70 ev Relative Abundance	Ion	70 ev Relative Abundance
Ni^+	77.4	$NiPF^+$	3.0
$NiPF_3^+$	100.0	$NiPF_3PF^+$	2.0
$Ni(PF_3)_2^+$	38.4		
$Ni(PF_3)_3^+$	14.5	NiF^+	9.9
$Ni(PF_3)_4^+$	3.4		
		NiP^+	4.0
$NiPF_2^+$	8.4		
$NiPF_3PF_2^+$	10.4	$NiPF_4^+$	10.4
$Ni(PF_3)_2PF_2^+$	12.8	$Ni(PF_3)_2^+$	0.5
$Ni(PF_3)_3PF_2^+$	0.7		
P^+	1.3	PF_2^+	27.3
PF^+	5.1	PF_3^+	7.4

isotopes necessary for the calculation of the total ion currents.

A comparison of the relative abundances in Table 10 for the ions formed from tetrakis(trifluorophosphine)nickel(0) and those produced from $Ni(CO)_4$ (59) indicates a significant similarity of these two molecules, although the $Ni(PF_3)_3^+$ and $Ni(PF_3)_4^+$ ions are much less abundant than the corresponding ions in the carbonyl compound. Additionally, no metal-containing ions possessing two positive charges were observed in the mass spectrum of $Ni(PF_3)_4$; this is in sharp contrast to the rather intense $NiCO^{++}$ (1.7% of the base peak) and $Ni(CO)_2^{++}$ (4.5% of the base peak) ions formed from $Ni(CO)_4$ (58). In $Ni(CO)_4$ the highest-occupied molecular orbital (e) arises principally from the 3d orbitals of the metal (39), i.e., are localized, and both the first and the second ionization potentials determined for the nickel-containing ions from $Ni(CO)_4$ support this (58). However, the absence of doubly-charged ions in the $Ni(PF_3)_4$ mass spectrum suggests that the Ni-PF_3 bond is different to some extent from the analogous bonding encountered in $Ni(CO)_4$. Since trifluorophosphine is the strongest π-acceptor neutral ligand known (32), it is expected to stabilize the lowest oxidation states of transition elements to a greater extent than any of the usual ligands. The greater stability of $Ni(PF_3)_4$ over $Ni(CO)_4$ confirms this. This greater stabilization, i.e., more extensive back-bonding, also effects the lowering of the energy of the highest occupied molecular orbitals and consequently requires more energy for the removal of the first and second electron from this orbital. The absence of doubly-charged ions supports this reasoning.

Degradation of the ligands is evidenced by the $NiPF_2^+$, $NiPF_3PF_2^+$, $Ni(PF_3)_2PF_2^+$, $Ni(PF_3)_3PF_2^+$, $NiPF^+$, $NiPF_3PF^+$, PF_2^+, PF^+ and P^+ ions. From the relative abundances of these species, one can conclude that this dissociation is less extensive than the elimination of the PF_3 group as a unit. Dugger (10) has investigated the fragmentation pattern of PF_3, which follows the initial detachment from the metal, and found it to occur by a stepwise elimination of the fluorine atoms as shown in Equation 33:

$$PF_3^+ \rightarrow PF_2^+ \rightarrow PF^+ \rightarrow P^+ \tag{33}$$

It is interesting to note that the PF_2^+ ion is much more abundant than the PF_3^+ or the PF^+, indicating a rapid dissociation of the PF_3^+ to PF_2^+ and a slower dissociation of PF_2^+ to PF^+. This mechanism is also indicated by the clastograms obtained by Dugger (10).

The dissociated fluorine atoms were not detected in the positive ion mass spectra, but are expected to be present in the negative ion mass spectra due to the high electron affinity of the fluorine atom.

2. Clastograms

A plot of fractional abundance as a function of electron energy gives valuable information as to the fragmentation scheme of a particular molecular ion. Clastograms determined for the five $Ni(PF_3)_n^+$ ions, where n = 0, 1, . . . 4, are shown in Figure 6. The same interpretation is applied in this study as that employed previously for $Ni(CO)_4$ (58), to show the consecutive unimolecular decomposition of $Ni(PF_3)_4^+$.

$$Ni(PF_3)_4^+ \rightarrow Ni(PF_3)_3^+ \rightarrow Ni(PF_3)_2^+ \rightarrow NiPF_3^+ \rightarrow Ni^+ \tag{34}$$

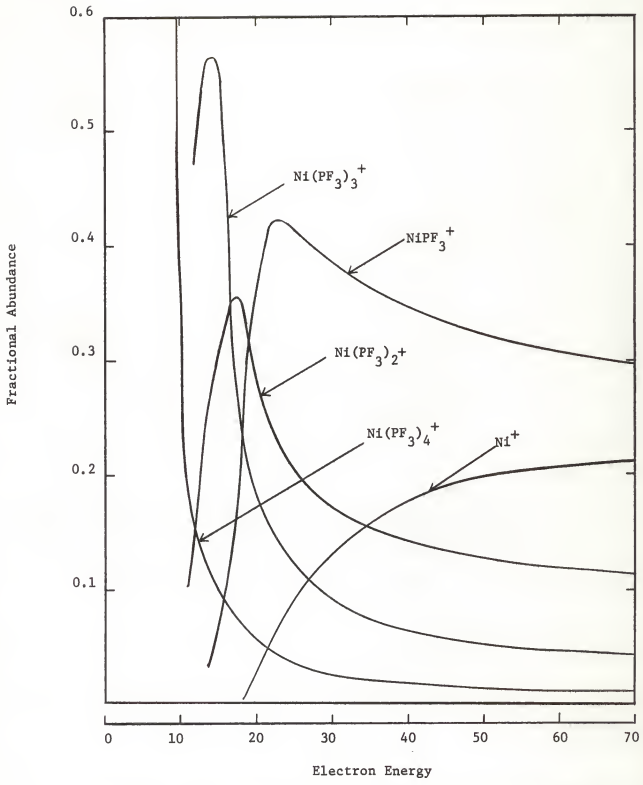

Figure 6. Clastogram of Tetrakis(trifluorophosphine)nickel(0).

As expected, the parent-molecule ion dominates at low energies and as the energy is increased, the fragment ions "grow-in" and maximize in order of increasing appearance potentials. This maximization indicates the further dissociation of the respective ions, $Ni(PF_3)_3^+$, $Ni(PF_3)_2^+$ and $NiPF_3^+$, to still smaller fragments and seems to be characteristic of the metal carbonyls as well as the trifluorophosphines, since the structures and bonding characteristics of these compounds are similar.

Other processes indicated by the complete clastogram study are: (i) $NiP_4F_{12}^+ \rightarrow NiP_4F_{11}^+ + F$, (ii) $NiP_3F_9^+ \rightarrow NiP_3F_8^+ + F$, (iii) $NiP_2F_6^+ \rightarrow NiP_2F_5^+ + F$ and (iv) $NiPF_3^+ \rightarrow NiPF_2^+ + F$. The clastograms in Figure 6 and 7 show that $Ni(PF_3)_4^+$, $Ni(PF_3)_3^+$, $Ni(PF_3)_2^+$ and $NiPF_3^+$ dissociate into simpler ions by at least two different paths:

$$Ni(PF_3)_4^+ \begin{cases} \nearrow Ni(PF_3)_3^+ + PF_3 \\ \searrow Ni(PF_3)_3PF_2^+ + F \end{cases} \quad (35)$$

$$Ni(PF_3)_3^+ \begin{cases} \nearrow Ni(PF_3)_2^+ + PF_3 \\ \searrow Ni(PF_3)_2PF_2^+ + F \end{cases} \quad (36)$$

$$Ni(PF_3)_2^+ \begin{cases} \nearrow NiPF_3^+ + PF_3 \\ \searrow NiPF_3PF_2^+ + F \end{cases} \quad (37)$$

and

$$NiPF_3^+ \begin{cases} \nearrow Ni^+ + PF_3 \\ \searrow NiPF_2^+ + F \end{cases} \quad (38)$$

Comparison of the fractional abundances of the $Ni(PF_3)_n^+$ and $Ni(PF_3)_nPF_2^+$ species in Figures 6 and 7 indicates that the $Ni(PF_3)_n^+$ ions are approximately ten times as abundant as the $Ni(PF_3)_n(PF_2)^+$ fragments. Therefore, the detachment of the PF_3 as a unit is preferred to the P-F bond dissociation. This is further evidenced by the electron energies at which the various

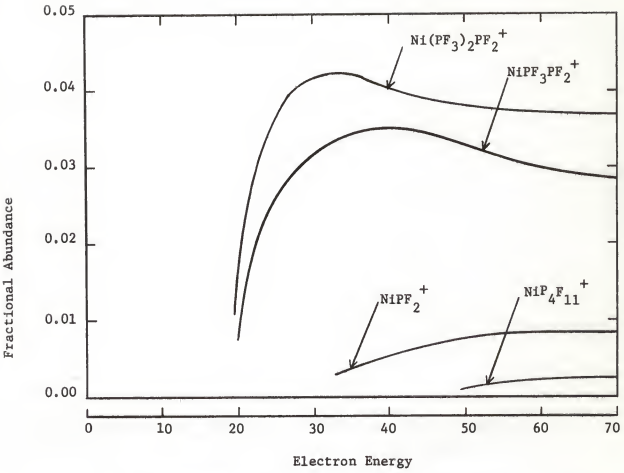

Figure 7. Clastogram for the Less Abundant Ions of Tetrakis-(trifluorophosphine)nickel(0).

species appear in the clastogram. The formation of the $Ni(PF_3)_n^+$ species, where n = 0,...4, occurs between 10 and 18 electron volts, while ions of the $Ni(PF_3)_nPF_2^+$ type, where n = 0,...3, appear above 20 electron volts. The appearance of the $NiP_4F_{11}^+$ ion (see Figure 7) would be expected just below 20 electron volts; however, its abundance was so low that it could not be detected in the mass spectrum at low electron energies.

3. Energetic Studies

To further substantiate the consecutive decomposition of $Ni(PF_3)_4$, the appropriate metastable transitions were obtained by the application of a retarding field on the multiplier stack of the Bendix time-of-flight mass spectrometer. The results are summarized in Table 2 and the transitions presented graphically in Figure 1. Metastable transitions were observed for all the steps in Equation 34 except $NiPF_3^+ \rightarrow Ni^+$. Transitions in the low mass regions are usually of such low intensity that the shift of the daughter ion (e.g., Ni^+) is impossible to detect (10).

In addition, a "metastable transition" for $NiP_4F_{11}^+ \rightarrow NiP_4F_{12}^+$ was detected and interpreted to be a collision phenomenon, i.e.,

$$NiP_4F_{11}^+ + Ni(PF_3)_4 \rightarrow Ni(PF_3)_4^+ + NiP_4F_{11} \qquad (39)$$

where the $NiP_4F_{11}^+$ ion collides with a neutral molecule, $Ni(PF_3)_4$, ejects an electron from its highest occupied molecular orbital, attracts this free electron and in essence undergoes a charge transfer reaction. Operating pressures in the ion source of the mass spectrometer, approximately 2-5 x 10^{-6} torr, are not particularly conducive to such reactions; however, this metastable study clearly indicates that this phenomenon occurs.

The appearance potentials, probable processess and the calculated heats of formation for the major ions in $Ni(PF_3)_4$ are listed in Table 11.

The ionization potential of $Ni(PF_3)_4$ is 8.7 $\pm$ 0.3 ev, a value much below the 11.5 ev required for the ionization of PF_3 (10). Therefore, the electron removed during ionization comes from a molecular orbital which is predominantly metal in character.

In order to determine the heat of formation of $Ni(PF_3)_4$ from the energetic data, the process

$$Ni(PF_3)_4 \rightarrow Ni^+ + 4PF_3 \qquad (40)$$

has been chosen as the most probable for the formation of the nickel ion. Assuming that the excess energy is the same as that involved in the formation of Ni^+ from $Ni(CO)_4$, and taking -219.6 kcal/mole as the heat of formation of PF_3 (10), a value of -948 kcal/mole is obtained for the heat of formation of tetrakis(trifluorophosphine)nickel(0). This value is within 20 kcal/mole of a value estimated using Franklin's method (16). Using this value of $\Delta H_f[Ni(PF_3)_4]$ and the processes listed in Table 11, the heats of formation of the other $Ni(PF_3)_n^+$ ions were calculated from Equation 4.

As successive PF_3 groups are added to a trifluorophosphine-nickel ion, the heat of formation becomes more negative, i.e., the addition of PF_3 groups to the nickel ion appears to stabilize the heat of formation. This increase in stability occurs at nearly constant increments as addition progresses. A similar trend has been observed in $Ni(CO)_4$ (58). The stabilization in $Ni(PF_3)_4$ is approximately 193 kcal/mole per PF_3 group greater than that found in its carbonyl analogue and again points to the stabilizing effect of the PF_3 group.

Table 11. Appearance Potentials and Heats of Formation of the Principal Positive Ions of Tetrakis(trifluorophosphine)-nickel(0).

Ion	Appearance Potential (ev)	Probable Process	ΔH_f^+ (ion) (kcal/mole)
$Ni(PF_3)_4^+$	8.7 ± 0.3	$Ni(PF_3)_4 \rightarrow Ni(PF_3)_4^+$	-747
$Ni(PF_3)_3^+$	9.7 ± 0.3	$\rightarrow Ni(PF_3)_3^+ + PF_3$	-505
$Ni(PF_3)_2^+$	11.4 ± 0.3	$\rightarrow Ni(PF_3)_2^+ + 2PF_3$	-246
$NiPF_3^+$	14.0 ± 0.3	$\rightarrow NiPF_3^+ + 3PF_3$	34
Ni^+	17.3 ± 0.3	$\rightarrow Ni^+ + 4PF_3$	330

C. Tetrakis(trifluorophosphine)cobalt(I)hydride

1. Mass Spectra

The 70 ev mass spectrum of $HCo(PF_3)_4$ is presented in Table 12. The base peak is the monotrifluorophosphine metal ion followed by the metal ion in abundance. Compared to the findings of Edgell and Risen (13), who observed a doublet of peaks separated by 28 atomic mass units in $HMn(CO)_5$, no such doublets were observed here, except for Co^+ and CoH^+. Since the time-of-flight instrument employed here is incapable of resolving the one atomic mass unit difference between a cobalt-trifluorophosphine and cobalt-trifluorophosphine-hydride ion, it is possible that both species were present, but were not identifiable. On several ions, the peak shapes definitely suggested an unresolved doublet, but no definite conclusion can be made as to the presence or absence of both fragments.

2. Clastograms

The clastograms for $HCo(PF_3)_4$ are shown in Figure 8. The curves behave as expected with the dominant $HCo(PF_3)_3^+$, $HCo(PF_3)_2^+$ and $HCoPF_3^+$ ions decreasing at low voltages while the parent molecule ion approaches the fractional abundance of unity. The slowly rising curves of Co^+ and CoH^+ with increasing electron energy are typical of the terminal process.

Table 12. Relative Abundances of the Principal Positive Ions from Tetrakis(trifluorophosphine)cobalt(I)-hydride.

Ion	70 ev Relative Abundance	Ion	70 ev Relative Abundance
Co^+	52.3	$HCoPF_3PF_2^+$	5.5
HCo^+	13.5	$HCo(PF_3)_2PF_2^+$	8.1
$CoPF_3^+$	100.0	$HCo(PF_3)_3PF_2^+$	0.4
$HCo(PF_3)_2^+$	40.3		
$HCo(PF_3)_3^+$	11.6	$CoPF^+$	1.7
$HCo(PF_3)_4^+$	5.4	$CoPF_2^+$	4.0
CoF^+	10.6	$CoPF_4^+$	4.9

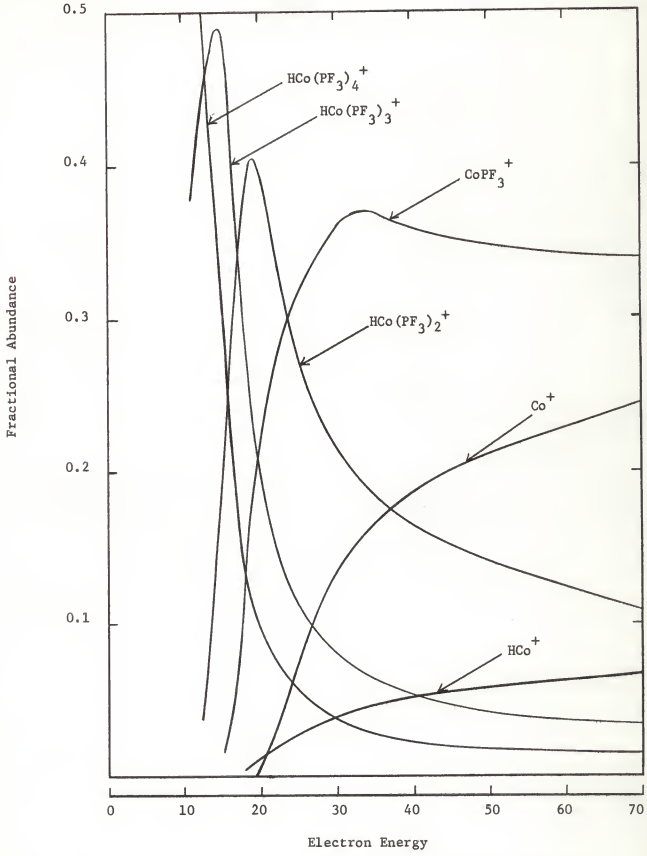

Figure 8. Clastogram of Tetrakis(trifluorophosphine)cobalt(I)-hydride.

3. Energetic Studies

For the prominent ions in tetrakis(trifluorophosphine)cobalt(I)-hydride, the appearance potentials, probable processes and heats of formation are summarized in Table 13.

The ionization potential was determined to be 9.2 $\pm$ 0.2 ev, a value which is again too low for a predominantly ligand-constituted molecular orbital. As in the case of the molybdenum and nickel compounds, the highest occupied molecular orbital must be composed largely of the 3d orbitals of the metal and therefore the electron removed during ionization must have been localized on the metal.

From the experimentally determined appearance potential of Co^+ and its heat of formation (33), the heat of formation of the parent molecule was calculated to be approximately -924 kcal/mole, including the correction made for excess energy possessed by such fragments in the mass spectrometer. As stated previously, ionization effected by electron impact is a vertical process as required by the Franck-Condon principle (14) and therefore the resulting ion may not always be in its ground state. As a result, ionization potentials measured by mass spectrometry are not infrequently somewhat greater than the spectroscopically determined values and consequently yield upper limits for the heat of formation of the parent molecule. From the results of previous studies (56), it has been found that the mass spectrometric value of $\Delta H_f(Co^+)$ is about 60 kcal/mole greater than the known spectroscopic value, and therefore this correction will yield values compatible with other determinations.

Table 13. Appearance Potentials and Heats of Formation of the Principal Positive Ions of Tetrakis(trifluorophosphine)-cobalt(I)hydride.

Ion	Appearance Potential (ev)	Probable Process	ΔH_f^+(ion) (kcal/mole)
$HCo(PF_3)_4^+$	9.2 ± 0.2	$HCo(PF_3)_4 \rightarrow HCo(PF_3)_4^+$	-712
$HCo(PF_3)_3^+$	10.4 ± 0.4	$\rightarrow HCo(PF_3)_3^+ + PF_3$	-475
$HCo(PF_3)_2PF_2^+$	15.4 ± 0.2	$\rightarrow HCo(PF_3)_2PF_2^+ + PF_2 + F_2$	-449
$HCo(PF_3)_2^+$	12.7 ± 0.2	$\rightarrow HCo(PF_3)_2^+ + 2PF_3$	-192
$HCoPF_3PF_2^+$	14.2 ± 0.2	$\rightarrow HCoPF_3PF_2^+ + 2PF_3 + F$	-176
$CoPF_3^+$	15.7 ± 0.3	$\rightarrow CoPF_3^+ + 3PF_3 + H$	45
$CoPF_2^+$	17.2 ± 0.3	$\rightarrow CoPF_2^+ + 3PF_3 + F + H$	60
Co^+	19.3 ± 0.5	$\rightarrow Co^+ + 4PF_3 + H$	347

The cobalt species in Table 13 indicate that the appearance potential increases with decreased PF_3 substitution on the metal, that is, greater energy increments are required to remove each successive PF_3 group. From the large values of the appearance potentials of $HCo(PF_3)_2PF_2^+$, $HCoPF_3PF_2^+$ and $CoPF_3^+$, one concludes that the rupture of the P-F bond requires more energy than the dissociation of a M-PF_3 bond.

V. SUMMARY

The principal positive ions of four trifluorophosphine-substituted transition metal carbonyls have been studied with a time-of-flight and high resolution mass spectrometers. No significant differences were noted in the two spectra. Ionization and appearance potentials were obtained for the major metal-containing ions and probable processes proposed for their formation, consistent with the measured threshold energies. Finally, heats of formation, all of which are new, have been calculated for these positively-charged ions.

The mass spectra of all the compounds studied indicate that the first PF_3 group is removed in preference to CO groups and that this is followed by the removal of the carbonyl and remaining PF_3 ligands. There is evidence of ligand dissociation prior to detachment from the central metal, but only to a small extent. No gross differences were observed in the fragmentation patterns of cis and trans-$Mo(CO)_4(PF_3)_2$, although doubly-charged ions were noted only in the trans isomer.

Clastograms for the major metal-containing ions show that fragmentation occurs by a consecutive unimolecular process, as in the carbonyls (56).

The ionization potentials measured for the molybdenum, nickel and cobalt compounds are similar or slightly higher than the ionization potential of the metal (38) and much lower than the ionization potential of the PF_3 and CO ligands (10,27); therefore, the electron removed during ionization is considered to be localized on the metal rather than on the ligand.

Assuming suitable reaction products for the metal ions fragmented from $Mo(CO)_5PF_3$, cis- and trans-$Mo(CO)_4(PF_3)_2$, $Ni(PF_3)_4$ and $HCo(PF_3)_4$, the calculated heats of formation are considerably higher than the accepted values (43). The discrepancies are generally larger than what could be assigned to kinetic energies, therefore these have been attributed to the formation of these ions in excited states. After appropriate corrections for the excited states, values consistent with the literature are obtained.

The results of this study show that trifluorophosphine-substituted transition metal carbonyls behave similarly to the unsubstituted carbonyls under electron impact. The relatively low abundance of the PF_3-containing species and the absence of doubly-charged ions in some of the compounds gives evidence of the difference in bonding tendencies of the CO and PF_3 ligands. On the basis of mass spectrometric evidence alone, the nature or the extent of this difference cannot be ascertained. The higher ionization potential of $Ni(PF_3)_4$ over $Ni(CO)_4$ supports the suggested stabilization of the zero oxidation state by the PF_3 group.

This investigation has provided some general information on the behavior of trifluorophosphine-substituted transition metal carbonyls under electron impact; however, further studies will be required to supplement and complete the now available information. These studies may include the determination of fragmentation patterns as a function of (i) the central metal atom and (ii) the oxidation state of the central metal atom. Ionization and appearance potentials of several more compounds could provide a more definite answer as to the bonding differences between CO and PF_3, as well as enable the acquisition of thermochemical information on ions not yet studied.

VI. ACKNOWLEDGMENTS

The author wishes to express her gratitude to Prof. R. W. Kiser for suggesting the problem and for his continued guidance, interest and patience.

Appreciation is also extended to Dr. R. J. Clark of Florida State University for supplying the compounds and to Dr. D. L. Dugger and Mr. R. E. Sullivan for their assistance with instrumental difficulties.

Acknowledgment is made to the United States Army for providing some financial assistance.

VII. LITERATURE CITED

1. H. G. Ang, J. S. Shannon and B. O. West, Chem. Commun., 1965, 10.

2. D. R. Bidinosti and N. S. McIntyre, Can. J. Chem., 45, 641 (1967).

3. K. Biemann, "Mass Spectrometry: Organic Chemical Applications", McGraw-Hill Book Company, Inc., New York, 1962, p. 370.

4. A. E. Cameron and D. F. Eggers, Jr., Rev. Sci. Instr., 19, 605 (1948).

5. B. Cantone, F. Grasso and S. Pignataro, J. Chem. Phys., 44, 3115 (1966).

6. R. J. Clark and E. O. Brimm, Inorg. Chem., 4, 651 (1965).

7. R. J. Clark and P. I. Hoberman, Inorg. Chem., 4, 1771 (1965).

8. "Digital Voltmeter", Model 3440A; manufactured by the Hewlett-Packard Co., Palo Alto, California.

9. J. G. Dillard, "Gaseous Inorganic Ion Decompositions: A Mass Spectrometric Study of Some Transition Metal Compounds," Doctoral Dissertation, Kansas State University, 1967, 179 pp.

10. D. L. Dugger, "Gaseous Ionic Decompositions of Selected Phosphorus Compounds," Doctoral Dissertation, Kansas State University, 1967, 259 pp.

11. D. L. Dugger and R. W. Kiser, J. Chem. Phys., accepted (1967).

12. K. Edgar, B. F. G. Johnson, J. Lewis, I. G. Williams and J. M. Wilson, J. Chem. Soc., (A), 1967, 379.

13. W. F. Edgell and W. M. Risen, Jr., J. Am. Chem. Soc., 88, 5451 (1966).

14. F. H. Field and J. L. Franklin, "Electron Impact Phenomena and the Properties of Gaseous Ions," Academic Press, Inc., New York, 1957, pp. 12, 249, 281, 305.

15. A. Foffani, S. Pignataro, B. Cantone and F. Grasso, Z. Physik. Chem. (Frankfurt), 45, 79 (1965).

16. J. L. Franklin, Ind. Eng. Chem., 41, 1070 (1949).

17. E. J. Gallegos, "Mass Spectrometric Investigation of Saturated Heterocyclics," Doctoral Dissertation, Kansas State University, 1962, 210 pp.

18. R. S. Gholke, Anal. Chem., 31, 535 (1959).

19. B. G. Hobrock, "Mass Spectrometric Investigation of Organic Mono-,Di- and Tri-Sulfides," Doctoral Dissertation, Kansas State University, 1964, 187 pp.

20. D. L. Hobrock, "Electron Impact Studies of Some Halogen-Containing Hydrocarbons," Doctoral Dissertation, Kansas State University, 1965, 142 pp.

21. J. W. S. Jamienson, J. V. Kingston and G. Wilkinson, Chem. Commun. 1966, 569.

22. B. F. G. Johnson, R. D. Johnston, J. Lewis, B. H. Robinson, Chem. Commun., 1966, 851.

23. B. F. G. Johnson, J. Lewis, I. G. Williams and J. M. Wilson, J. Chem. Soc., (A), 1967, 338.

24. H. S. Katzenstein and S. S. Friedland, Rev. Sci. Instr., 26, 324, (1955).

25. A. B. King and F. A. Long, J. Chem. Phys., 29, 374 (1958).

26. R. B. King, "Mass Spectra of Metal Carbonyl Complexes of Tris-(Dimethylamino)phosphine," presented before the Division of Inorganic Chemistry, 153d National ACS Meeting, Miami Beach, Florida April 10-14, 1967.

27. R. W. Kiser, "Introduction to Mass Spectrometry and Its Applications", Prentice-Hall, Inc., Englewood Cliffs, New Jersey, 1965, 365 pp.

28. R. W. Kiser, "Tables of Ionization Potentials," U. S. Atomic Energy Commission, TID-6142, June 20, 1960; and supplements.

29. R. W. Kiser and E. J. Gallegos, J. Phys. Chem., 66, 947 (1962).

30. R. W. Kiser, M. A. Krassoi and R. J. Clark, J. Am. Chem. Soc., 89, 3653 (1967).

31. R. W. Kiser and R. E. Winters, "A Kinetic Interpretation of Clastograms," presented before the Division of Physical Chemistry at the 152nd National ACS Meeting, New York, September 11-16 1966.

32. Th. Kruck, Angew. Chem., (Intern. Ed.), 6, 53, (1967).

33. W. M. Latimer, "The Oxidation States of the Elements and Their Potentials in Aqueous Solutions," 2nd Edition, Prentice-Hall, Inc., Englewood Cliffs, New Jersey, 1952, 392 pp.

34. J. L. Lewis, A. R. Manning, J. R. Miller and J. M. Wilson, J. Chem. Soc., (A), 1966, 1663.

35. F. P. Lossing, A. W. Tickner and W. A. Bryce, J. Chem. Phys., 19, 1254 (1951).

36. C. E. Melton and W. H. Hamil, J. Chem. Phys., 41, 546 (1964).

37. C. E. Melton and W. H. Hamil, "Techniques for Studying Appearance Potentials (RPD) and Ion-Molecule Reactions with the Bendix TOF Mass Spectrometer," Notre Dame Report, 1963.

38. C. E. Moore, "Atomic Energy Levels," National Bureau of Standards Circular No. 467, volumes 1, 2, and 3, U. S. Government Printing Office, Washington, D. C. 1949, 1952, 1958.

39. W. C. Nieuwpoort, "Charge Distribution and Chemical Bonding in the Metal Carbonyls $Ni(CO)_4$, $(Co(CO)_4)^-$, and $(Fe(CO)_4)^=$, a Non Empirical Approach," Doctoral Dissertation, University of Amsterdam, 1965 Philips Res. Repts. Suppl., 1965, No. 6. 104 pp.

40. S. Pignataro, A. Foffani, F. Grasso and B. Cantone, Z. Physik. Chem. (Frankfurt), 47, 106 (1965).

41. W. C. Price and T. R. Passmore, Discussions Faraday Soc., 35, 232 (1963).

42. M. G. Rhomberg and B. B. Owen, J. Am. Chem. Soc., 73, 5904 (1961).

43. R. D. Rossini, D. D. Wagman, W. H. Evans, S. Levine and I. Jaffe, "Selected Values of Chemical Thermodynamic Properties," National Bureau of Standards Circular 500, U. S. Government Printing Office, Washington, D. C. 1962, 1268 pp.

44. F. E. Saalfeld, M. V. McDowell, Surinder Gondal and A. G. MacDiarmid, "The Mass Spectra of Three Cobalt Carbonyl Hydrides," presented at The Fifteenth Annual Conference on Mass Spectrometry and Allied Topics, ASTM Committee E-14 on Mass Spectrometry, Denver, Colorado May 14-19, 1967.

45. S. M. Schildcrout, G. A. Pressley, Jr., and F. E. Stafford, J. Am. Chem. Soc., 89, 1617 (1967).

46. L. A. Shadoff, "Analyses of Ionization Efficiency Curves and Multiple Ionization Processes," Doctoral Dissertation, Kansas State University, 1966.

47. "Sonblaster" Ultrasonic Generator, Series 600; manufactured by The Narda Ultrasonic Corp., Westbury, L. I., New York.

48. R. H. Vought, Phys. Rev., 71, 93 (1947).

49. Y. Wada, "Mass Spectrometric Investigation of Some Inorganic and Organic Phosphorus Compounds," Doctoral Dissertation, Kansas State University, 1964, 164 pp.

50. D. D. Wagman, W. H. Evans, I. Halow, V. B. Parker, S. M. Bailey and R. H. Schumm, "Selected Values of Chemical Thermodynamic Properties. Part I. Tables for the 1-st Twenty-three Elements in the Standard Order of Arrangement," National Bureau of Standards Technical Note 270-1, U. S. Government Printing Office, Washington, D. C., 1965.

51. J. W. Warren, Nature, 165, 810 (1950).

52. J. H. Weber, "Mass Spectrometric Investigations of Some Organic Esters," Doctoral Dissertation, Kansas State University, 1966, 156 pp.

53. W. C. Wiley, Science, 124, 817, (1956).

54. W. C. Wiley and I. H. McLaren, Rev. Sci. Instr., 26, 1150 (1955).

55. G. Wilkinson, J. Am. Chem. Soc., 73, 550 (1951).

56. R. E. Winters, "A Mass Spectrometric Study of Some Organometallic Compounds," Doctoral Dissertation, Kansas State University, 1965, 170 pp.

57. R. E. Winters and J. H. Collins, J. Phys. Chem., 70, 2057 (1966).

58. R. E. Winters and R. W. Kiser, Inorg. Chem., 3, 699 (1964).

59. R. E. Winters and R. W. Kiser, Inorg. Chem., 4, 157 (1965).

60. R. E. Winters and R. W. Kiser, J. Chem. Phys., 44, 1964 (1966).

61. R. E. Winters and R. W. Kiser, J. Phys. Chem., 69, 1618 (1965).

62. R. E. Winters and R. W. Kiser, J. Phys. Chem., 69, 3198 (1965).

63. R. E. Winters and R. W. Kiser, J. Phys. Chem., 70, 1680 (1966).

64. R. E. Winters and R. W. Kiser, J. Organometal. Chem., (Amsterdam), 4, 190 (1965).

65. M. M. Wolff and W. E. Stevens, Rev. Sci. Instr., 24, 616 (1953).

APPENDICES

Appendix A. The method by which the masses of the daughter ions in the metastable transitions in the time-of-flight mass spectrometer are calculated is presented here. Equations leading to the final mass of the daughter ions are also given.

Appendix B. To enable the calculation of the heats of formation for ions formed in the mass spectrometer, thermochemical values for certain molecules, ions or radicals, indicated by the proposed processes, are necessary. These values and their sources are tabulated in this appendix.

Appendix C. The ionic species formed in the mass spectrometer, molecules from which they originate, and their heats of formation are summarized in this section. To provide a basis for comparison with previous studies, the heats of formation of the various ions reported in the literature are also included wherever possible.

Appendix A. Tabulation of Data for Metastable Transition Calculations Using the Bendix Time-of-Flight Mass Spectrometer.

Table 14. $410^{+} \rightarrow 322^{+} + 88$ Metastable Transition in Tetrakis(trifluorophosphine)nickel(0).

A. Calibration of Chart Paper:

$\Delta t = 100\ (\sqrt{410} - \sqrt{28})/7.6064 \times 10^{7} = 19.67$ sec; $\Delta d = 1707$ mm; $\Delta t/\Delta d = 0.01152$ μsec/mm

B. Calculation of $t_4°$:

$t_4° = [(165.97)(410)/57.8569 \times 10^{14})]^{½} = 3.4295$ μsec.

C. Least Squares Treatment:

Δl	t_s	t_4	t_4^2	$1/t_4^2$	V_s	$[1/t_4]^2$	V_s'	$(V_s')^2$	$V_s'[1/t_4]^2$
33.0	0.3802	3.8097	14.5138	0.0689	2600	0.0180	550	302550	9.900
39.5	0.4550	3.8845	15.0893	0.0663	2500	0.0154	450	202500	6.930
49.0	0.5645	3.9940	15.9520	0.0627	2400	0.0118	350	122500	4.130
54.5	0.6278	4.0573	16.4617	0.0607	2300	0.0098	250	62500	2.450
58.0	0.7834	4.2129	17.7486	0.0563	2200	0.0054	150	22500	0.810
80.0	0.9216	4.3511	18.9321	0.0528	2100	0.0019	50	2500	0.095
95.5	1.1002	4.5297	20.5182	0.0487	2000	-0.0022	-50	2500	0.110
108	1.2442	4.6737	21.8435	0.0458	1900	-0.0051	-150	22500	0.765
122	1.4054	4.8349	23.3763	0.0428	1800	-0.0081	-250	62500	2.025
141	1.6243	5.0538	25.5409	0.0392	1700	-0.0117	-350	122500	4.095
166	1.9123	5.3418	28.5348	0.0350	1600	-0.0159	-450	202500	7.155
192	2.2118	5.6413	31.8243	0.0314	1500	-0.0195	-550	302500	10.725
			Sum:	0.6106	24600	-0.0002	0	1430000	49.190
			Avg:	0.0509	2050				

D. Calculation of m from Slope:

$m = (578.569)\ (100)/(165.97)(1.032) = 337.8$

E. Calculation of m from Intercept:

$0.0509 \times 100/(0.0343986) = 1480$; $V_s° = 2050 - 1480 = 570$; $570/3000 = 0.190$

$(1 - 0.190) = 0.810$; $m = (410)\ (0.810) - 332$

F. Average of D and E: 335

Table 15. $322^{+} \rightarrow 234^{+} + 88$ Metastable Transition in Tetrakis(trifluorophosphine)nickel(0).

A. Calibration of Chart Paper:

$\Delta t = 100\ (\sqrt{410} - \sqrt{28})/7.6064 \times 10^{7} = 19.67$ μsec; d = 1707 mm; $\Delta t/\Delta d = 0.01152$ μsec/mm

B. Calculation of $t_4°$

$t_4° = [(165.97)\ (322)/57.8569 \times 10^{14})]^{\frac{1}{2}} = 3.0392$ μsec.

C. Least Squares Treatment:

Δl	t_s	t_4	t_4^2	$1/t_4^2$	V_s	$[1/t_4^2]'$	V_s'	$(V_s')^2$	$[V_s'\ 1/t_4^2]'$
38.0	0.4378	3.4770	12.08953	0.0827	2500	0.0220	450	202500	9.900
46.0	0.5299	3.5691	12.73847	0.0785	2400	0.0178	350	122500	6.230
57.0	0.6566	3.6958	13.65894	0.0732	2300	0.0125	250	62500	3.125
70.5	0.8122	3.8514	14.83328	0.0674	2200	0.0067	150	22500	1.005
82.0	0.9446	3.9838	15.87066	0.0630	2100	0.0023	50	2500	0.115
97.0	1.1174	4.1566	17.27732	0.0579	2000	-0.0028	-50	2500	0.140
112	1.2902	4.3294	18.74370	0.0534	1900	-0.0073	-150	22500	1.095
131	1.5091	4.5483	20.68703	0.0483	1800	-0.0124	-250	62500	3.100
150	1.7280	4.7672	22.72620	0.0440	1700	-0.0167	-350	122500	5.845
176	2.0275	5.0667	25.67145	0.0390	1600	-0.0217	-450	202500	9.765
			Sum:	0.6074	20500	+0.0004	0	825000	40.320
			Avg:	0.0607	2050				

D. Calculation of m from Slope:

$m = (578.569)\ (100)/(165.97)(1.46618) = 237.8$

E. Calculation of m from Intercept:

$(0.06074)\ (1000)/(0.048873) = 1243$; $V_s° = 2050 - 1243 = 807$; $807/3000 = 0.269$

F. Average of D and E: 236

Table 16. $234^+ \rightarrow 146^+ + 88$ Metastable Transition in Tetrakis(trifluorophosphine)nickel(0).

A. Calibration of Chart Paper:

$t = 100 (\sqrt{410} - \sqrt{28})/7.6064 \times 10^7 = 19.67$ μsec; d = 1707 mm; $\Delta t/\Delta d = 0.01152$ μsec/mm

B. Calculation of $t_4°$:

$t_4° = [(167.97)\ (234)/57.8569 \times 10^{14})]^{½} = 2.5909$ μsec.

C. Least Squares Treatment:

Δl	t_s	t_4	t_4^2	$1/t_4^2$	v_s	$[1/t_4^2]'$	v_s	$(v_s')^2$	$v_s'[1/t_4^2]'$
33.0	0.3802	2.9711	8.82744	0.1133	2600	0.03345	450	202500	15.0525
39.0	0.4493	3.0402	9.24282	0.1082	2500	0.02835	350	122500	9.9225
50.0	0.5760	3.1669	10.02926	0.0997	2400	0.01985	250	62500	4.9625
63.0	0.7258	3.3167	11.00050	0.0909	2300	0.01105	150	22500	1.6575
76.0	0.8755	3.4664	12.01593	0.0832	2200	0.00335	50	2500	0.1675
89.0	1.0253	3.6162	13.07690	0.0765	2100	-0.00335	-50	2500	0.1675
108	1.2442	3.8351	14.70799	0.0680	2000	-0.01105	-150	22500	1.7775
127	1.4630	4.0539	16.43411	0.0608	1900	-0.01905	-250	62500	4.7625
155	1.7856	4.3765	19.15375	0.0522	1800	-0.02765	-350	122500	9.6775
181	2.0851	4.6760	21.86498	0.0457	1700	-0.03415	-450	202500	15.3675
			Sum:	0.7985	21500	0.00000	0	825000	63.5150
			Avg:	0.0799	2150				

D. Calculation of m from Slope:

$m = (578.569)(100)/(165.97)(2.30964) = 150.9$

E. Calculation of m from Intercept:

$(0.07985)\ (1000)/(0.0769879) = 1037$; $v_s° = 2150 - 1037 = 1113$; $1113/3000 = 0.371$

$(1-0.371) = 0.629$; $m = (234)\ (0.629) = 147.2$

F. Average of D and E: 149

Table 17. $391^{+} + 410 \rightarrow 410^{+} + 391$ Charge Exchange in Tetrakis(trifluorophosphine)nickel(0).

A. Calibration of Chart Paper:

$t = 100(\sqrt{410} - \sqrt{391})/7.6064 \times 10^{7} = 0.6244$ μsec x 1 mm/0.01152 μsec = 54.2 mm

B. Calculation of $t_4°$:

C. Least Squares Treatment:

Δl	t_s	t_4	t_4^2	$1/t_4^2$	V_s	$[1/t_4^2]'$	V_s'	$(V_s')^2$	$V_s'\,[1/t_4^2]'$
24.5	0.2822	3.6313	13.18634	0.0758	2600	0.01515	550	302500	8.3325
31.5	0.3629	3.7120	13.77894	0.0726	2500	0.01195	450	202500	5.3775
37.0	0.4262	3.7753	14.25289	0.0702	2400	0.00955	350	122500	3.3425
40.0	0.4608	3.8099	14.51534	0.0689	2300	0.00825	250	62500	2.0625
50.0	0.5760	3.9251	15.40641	0.0649	2200	0.00425	150	22500	0.6375
58.0	0.6682	4.0173	16.13870	0.0620	2100	0.00135	50	2500	0.0675
65.0	0.7488	4.0979	16.79278	0.0595	2000	-0.00115	-50	2500	0.0575
74.0	0.8525	4.2016	17.65344	0.0566	1900	-0.00405	-150	22500	0.6075
82.0	0.9446	4.2937	18.43586	0.0542	1800	-0.00645	-250	62500	1.6125
94.0	1.0829	4.4320	19.64262	0.0509	1700	-0.00975	-350	122500	3.4125
108	1.2442	4.5933	21.09840	0.0474	1600	-0.01325	-450	202500	5.9625
119	1.3790	4.7200	22.27840	0.0449	1500	-0.01575	-550	302500	8.6625
			Sum:	0.7279	24600	-0.001	0	1430000	40.1350
			Avg:	0.0607	2050				

D. Calculation of m from Slope:

$m = (578.569)(100)/(165.97)(0.8420) = 414$

E. Calculation of m from Intercept:

$(0.06066)\ (100)/(0.028066) = 2161$; $V_s° = 2050 - 2161 = -111$; $-111/3000 = -0.037$

$(1 + 0.037) = 1.037$; $m = (1.037)(301) = 405.5$

F. Average of D and E: 410

Appendix B. Heats of Formation (in kcal/mole) for the Molecules, Atoms, Ions and Radicals Used in the Thermochemical Calculations.

Species	State	ΔH_f (kcal/mole)	Reference
Co^+	g	287	33
CO	g	14.01	27
F	g	18.88	50
H	g	52.095	50
$Mo(CO)_3^+$	g	177	59
$Mo(CO)_2^+$	g	247	59
$MoCO^+$	g	331	59
Ni^+	g	330	58
PF_2	g	-120	10
PF_3	g	-219.6	50
$Ni(PF_3)_4$	g	-948	30, a
$HCo(PF_3)_4$	g	-924	a
$Mo(CO)_5PF_3$	g	-400	a
cis-$Mo(CO)_4(PF_3)_2$	g	-595	a
trans-$Mo(CO)_4(PF_3)_2$	g	-595	a
$MoCO(PF_3)_5$	g	-1175	a
$Mo(PF_3)_6$	g	-1365	a

a) estimated in this work; see text.

Appendix C. Tabulation of Heat of Formation (in kcal/mole) of Ionic Species Studied.

Ionic Species	ΔH_f (kcal/mole) This work	Other studies	Literature Reference
Mo^+			
$Mo(CO)_5PF_3$	385		
cis-$Mo(CO)_4(PF_3)$	376		
trans-$Mo(CO)_4(PF_3)$	365		
$Mo(CO)_6$		369	2
		362	15
		417	56
Mo		327	33
$MoCO^+$			
$Mo(CO)_5PF_3$	313		
cis-$Mo(CO)_4(PF_3)_2$	311		
trans-$Mo(CO)_4(PF_3)_2$	311		
$Mo(CO)_6$		278	2
		278	15
		331	56
$Mo(CO)_2^+$			
$Mo(CO)_5PF_3$	242		
cis-$Mo(CO)_4(PF_3)_2$	248		
trans-$Mo(CO)_4(PF_3)_2$	241		
$Mo(CO)_6$		215	2
		208	15
		247	56
$Mo(CO)_3^+$			
$Mo(CO)_5PF_3$	184		
cis-$Mo(CO)_4(PF_3)_2$	189		
trans-$Mo(CO)_4(PF_4)_2$	189		
$Mo(CO)_6$		151	2
		147	15
		177	56
$Mo(CO)_4^+$			
$Mo(CO)_5PF_3$	116		
trans-$Mo(CO)_4(PF_3)$	128		
$Mo(CO)_6$		87	2
		95	15
		109	56

Appendix C. continued.

Ionic Species	ΔH_f (kcal/mole) This work	Other studies	Literature Reference
$Mo(CO)_2PF_3^+$			
cis-$Mo(CO)_4(PF_3)_2$	-11		
trans-$Mo(CO)_4(PF_3)_2$	-5		
$Mo(CO)_3PF_3^+$			
cis-$Mo(CO)_4(PF_3)_2$	-72		
trans-$Mo(CO)_4(PF_3)_2$	-70		
$Mo(CO)_5^+$			
$Mo(CO)_5PF_3$	80	28	2
$Mo(CO)_6$		29	15
$Mo(CO)_4(PF_3)_2^+$			
cis-$Mo(CO)_4(PF_3)_2$	-390		
trans-$Mo(CO)_4(PF_3)_2$	-392		
$Mo(CO)_5PF_3^+$			
$Mo(CO)_5PF_3$	197		
Ni^+			
$Ni(PF_3)_4$	330		
$Ni(CO)_4$		309	2
		293	45
		293	15
		330	56
Ni		279	33
$NiPF_3^+$			
$Ni(PF_3)_4$	34		
$Ni(PF_3)_2^+$			
$Ni(PF_3)_4$	-246		
$Ni(PF_3)_3^+$			
$Ni(PF_3)_4$	-505		
$Ni(PF_3)_4^+$			
$Ni(PF_3)_4$	-747		

Appendix C. continued.

Ionic Species	ΔH_f (kcal/mole) This work	ΔH_f (kcal/mole) Other Studies	Literature Reference
Co^+			
$HCo(PF_3)_4$	347		
$Co_2(CO)_8$		347	56
Co		287	33
$CoPF_2^+$			
$HCo(PF_3)_4$	60		
$CoPF_3^+$			
$HCo(PF_3)_4$	45		
$HCo(CO)_3PF_3$		8	44
$HCo(CO)_2(PF_3)_2$		14	44
$HCoCO(PF_3)_3$		6	44
$HCoPF_3PF_2^+$			
$HCo(PF_3)_4$	-176		
$HCo(PF_3)_2^+$			
$HCo(PF_3)_4$	-192		
$HCoCO(PF_3)$		-240	44
$HCo(PF_3)_2PF_2^+$			
$HCo(PF_3)_4$	-449		
$HCO(PF_3)_3^+$			
$HCo(PF_3)_4$	-475		
$HCoCO(PF_3)_3$		-500	44
$HCo(PF_3)_4^+$			
$HCo(PF_3)_4$	-712		

A MASS SPECTROMETRIC STUDY OF SOME TRIFLUOROPHOSPHINE-SUBSTITUTED TRANSITION METAL CARBONYLS

by

MARIA ANN KRASSOI

B. S., Notre Dame College, 1965

AN ABSTRACT OF A MASTER'S THESIS

submitted in partial fulfillment of the

requirements for the degree

MASTER OF SCIENCE

Department of Chemistry

KANSAS STATE UNIVERSITY
Manhattan, Kansas

1968

The principal positive ions of four trifluorophosphine-substituted transition metal carbonyls have been studied on a time-of-flight and a high resolution mass spectrometer. No significant differences were noted in the two spectra. From its isotopic abundances, a tungsten impurity was identified in the high resolution mass spectra of some of the molybdenum compounds. Relative abundances are comparable to those of the carbonyl analogues, and indicate the preferential removal of the first PF_3, followed by the removal of the CO and remaining phosphorous trifluorides in succession. There was evidence of ligand dissociation prior to detachment from the central metal.

Clastogram studies show that fragmentation occurs by a consecutive unimolecular process.

Ionization potentials measured for the three transition metal compounds are similar to the ionization potential of the metal, but much lower than the ionization potential of the ligands. Therefore, the electron removed during ionization is considered to have been localized on the metal rather than on the ligand.

The calculated heats of formation are considerably higher than the accepted values, and these discrepancies are much greater than what could be due to kinetic energies. Therefore, the formation of the ions in excited states depending on the original electronic configuration of the molecule is suggested to be the cause of the high values.

The experimental data compiled in this study shows that the nature of the M-CO and M-PF_3 bonds are somewhat different, although unsubstituted and trifluorophosphine-substituted transition metal carbonyls behave similarly under electron impact.